32ND INTERNATIONAL COSMIC RAY CONFERENCE, BEIJING 2011

The IceCube Neutrino Observatory II:

All Sky Searches: Atmospheric, Diffuse and EHE

THE ICECUBE COLLABORATION

Keywords: *IceCube, neutrino astronomy, AGN, GZK mechanism, cosmogenic neutrinos, atmospheric neutrinos, cascades, energy spectrum, regularized unfolding, TRUEE*

32ND INTERNATIONAL COSMIC RAY CONFERENCE, BEIJING 2011

THE ICECUBE COLLABORATION

R. ABBASI[28], Y. ABDOU[22], T. ABU-ZAYYAD[33], M. ACKERMANN[39], J. ADAMS[16], J. A. AGUILAR[28], M. AHLERS[32], M. M. ALLEN[36], D. ALTMANN[1], K. ANDEEN[28,a], J. AUFFENBERG[38], X. BAI[31,b], M. BAKER[28], S. W. BARWICK[24], R. BAY[7], J. L. BAZO ALBA[39], K. BEATTIE[8], J. J. BEATTY[18,19], S. BECHET[13], J. K. BECKER[10], K.-H. BECKER[38], M. L. BENABDERRAHMANE[39], S. BENZVI[28], J. BERDERMANN[39], P. BERGHAUS[31], D. BERLEY[17], E. BERNARDINI[39], D. BERTRAND[13], D. Z. BESSON[26], D. BINDIG[38], M. BISSOK[1], E. BLAUFUSS[17], J. BLUMENTHAL[1], D. J. BOERSMA[1], C. BOHM[34], D. BOSE[14], S. BÖSER[11], O. BOTNER[37], A. M. BROWN[16], S. BUITINK[14], K. S. CABALLERO-MORA[36], M. CARSON[22], D. CHIRKIN[28], B. CHRISTY[17], F. CLEVERMANN[20], S. COHEN[25], C. COLNARD[23], D. F. COWEN[36,35], A. H. CRUZ SILVA[39], M. V. D'AGOSTINO[7], M. DANNINGER[34], J. DAUGHHETEE[5], J. C. DAVIS[18], C. DE CLERCQ[14], T. DEGNER[11], L. DEMIRÖRS[25], F. DESCAMPS[22], P. DESIATI[28], G. DE VRIES-UITERWEERD[22], T. DEYOUNG[36], J. C. DÍAZ-VÉLEZ[28], M. DIERCKXSENS[13], J. DREYER[10], J. P. DUMM[28], M. DUNKMAN[36], J. EISCH[28], R. W. ELLSWORTH[17], O. ENGDEGÅRD[37], S. EULER[1], P. A. EVENSON[31], O. FADIRAN[28], A. R. FAZELY[6], A. FEDYNITCH[10], J. FEINTZEIG[28], T. FEUSELS[22], K. FILIMONOV[7], C. FINLEY[34], T. FISCHER-WASELS[38], B. D. FOX[36], A. FRANCKOWIAK[11], R. FRANKE[39], T. K. GAISSER[31], J. GALLAGHER[27], L. GERHARDT[8,7], L. GLADSTONE[28], T. GLÜSENKAMP[39], A. GOLDSCHMIDT[8], J. A. GOODMAN[17], D. GÓRA[39], D. GRANT[21], T. GRIESEL[29], A. GROSS[16,23], S. GRULLON[28], M. GURTNER[38], C. HA[36], A. HAJ ISMAIL[22], A. HALLGREN[37], F. HALZEN[28], K. HAN[39], K. HANSON[13,28], D. HEINEN[1], K. HELBING[38], R. HELLAUER[17], S. HICKFORD[16], G. C. HILL[28], K. D. HOFFMAN[17], A. HOMEIER[11], K. HOSHINA[28], W. HUELSNITZ[17,c], J.-P. HÜLSS[1], P. O. HULTH[34], K. HULTQVIST[34], S. HUSSAIN[31], A. ISHIHARA[15], E. JACOBI[39], J. JACOBSEN[28], G. S. JAPARIDZE[4], H. JOHANSSON[34], K.-H. KAMPERT[38], A. KAPPES[9], T. KARG[38], A. KARLE[28], P. KENNY[26], J. KIRYLUK[8,7], F. KISLAT[39], S. R. KLEIN[8,7], J.-H. KÖHNE[20], G. KOHNEN[30], H. KOLANOSKI[9], L. KÖPKE[29], S. KOPPER[38], D. J. KOSKINEN[36], M. KOWALSKI[11], T. KOWARIK[29], M. KRASBERG[28], T. KRINGS[1], G. KROLL[29], N. KURAHASHI[28], T. KUWABARA[31], M. LABARE[14], K. LAIHEM[1], H. LANDSMAN[28], M. J. LARSON[36], R. LAUER[39], J. LÜNEMANN[29], J. MADSEN[33], A. MAROTTA[13], R. MARUYAMA[28], K. MASE[15], H. S. MATIS[8], K. MEAGHER[17], M. MERCK[28], P. MÉSZÁROS[35,36], T. MEURES[13], S. MIARECKI[8,7], E. MIDDELL[39], N. MILKE[20], J. MILLER[37], T. MONTARULI[28,d], R. MORSE[28], S. M. MOVIT[35], R. NAHNHAUER[39], J. W. NAM[24], U. NAUMANN[38], D. R. NYGREN[8], S. ODROWSKI[23], A. OLIVAS[17], M. OLIVO[10], A. O'MURCHADHA[28], S. PANKNIN[11], L. PAUL[1], C. PÉREZ DE LOS HEROS[37], J. PETROVIC[13], A. PIEGSA[29], D. PIELOTH[20], R. PORRATA[7], J. POSSELT[38], P. B. PRICE[7], G. T. PRZYBYLSKI[8], K. RAWLINS[3], P. REDL[17], E. RESCONI[23,e], W. RHODE[20], M. RIBORDY[25], M. RICHMAN[17], J. P. RODRIGUES[28], F. ROTHMAIER[29], C. ROTT[18], T. RUHE[20], D. RUTLEDGE[36], B. RUZYBAYEV[31], D. RYCKBOSCH[22], H.-G. SANDER[29], M. SANTANDER[28], S. SARKAR[32], K. SCHATTO[29], T. SCHMIDT[17], A. SCHÖNWALD[39], A. SCHUKRAFT[1], A. SCHULTES[38], O. SCHULZ[23,f], M. SCHUNCK[1], D. SECKEL[31], B. SEMBURG[38], S. H. SEO[34], Y. SESTAYO[23], S. SEUNARINE[12], A. SILVESTRI[24], G. M. SPICZAK[33], C. SPIERING[39], M. STAMATIKOS[18,g], T. STANEV[31], T. STEZELBERGER[8], R. G. STOKSTAD[8], A. STÖSSL[39], E. A. STRAHLER[14], R. STRÖM[37], M. STÜER[11], G. W. SULLIVAN[17], Q. SWILLENS[13], H. TAAVOLA[37], I. TABOADA[5], A. TAMBURRO[33], A. TEPE[5], S. TER-ANTONYAN[6], S. TILAV[31], P. A. TOALE[2], S. TOSCANO[28], D. TOSI[39], N. VAN EIJNDHOVEN[14], J. VANDENBROUCKE[7], A. VAN OVERLOOP[22], J. VAN SANTEN[28], M. VEHRING[1], M. VOGE[11], C. WALCK[34], T. WALDENMAIER[9], M. WALLRAFF[1], M. WALTER[39], CH. WEAVER[28], C. WENDT[28], S. WESTERHOFF[28], N. WHITEHORN[28], K. WIEBE[29], C. H. WIEBUSCH[1], D. R. WILLIAMS[2], R. WISCHNEWSKI[39], H. WISSING[17], M. WOLF[23], T. R. WOOD[21], K. WOSCHNAGG[7], C. XU[31], D. L. XU[2], X. W. XU[6], J. P. YANEZ[39], G. YODH[24], S. YOSHIDA[15], P. ZARZHITSKY[2], M. ZOLL[34]

[1] *III. Physikalisches Institut, RWTH Aachen University, D-52056 Aachen, Germany*
[2] *Dept. of Physics and Astronomy, University of Alabama, Tuscaloosa, AL 35487, USA*
[3] *Dept. of Physics and Astronomy, University of Alaska Anchorage, 3211 Providence Dr., Anchorage, AK 99508, USA*
[4] *CTSPS, Clark-Atlanta University, Atlanta, GA 30314, USA*
[5] *School of Physics and Center for Relativistic Astrophysics, Georgia Institute of Technology, Atlanta, GA 30332, USA*
[6] *Dept. of Physics, Southern University, Baton Rouge, LA 70813, USA*
[7] *Dept. of Physics, University of California, Berkeley, CA 94720, USA*
[8] *Lawrence Berkeley National Laboratory, Berkeley, CA 94720, USA*
[9] *Institut für Physik, Humboldt-Universität zu Berlin, D-12489 Berlin, Germany*
[10] *Fakultät für Physik & Astronomie, Ruhr-Universität Bochum, D-44780 Bochum, Germany*
[11] *Physikalisches Institut, Universität Bonn, Nussallee 12, D-53115 Bonn, Germany*
[12] *Dept. of Physics, University of the West Indies, Cave Hill Campus, Bridgetown BB11000, Barbados*
[13] *Université Libre de Bruxelles, Science Faculty CP230, B-1050 Brussels, Belgium*
[14] *Vrije Universiteit Brussel, Dienst ELEM, B-1050 Brussels, Belgium*
[15] *Dept. of Physics, Chiba University, Chiba 263-8522, Japan*
[16] *Dept. of Physics and Astronomy, University of Canterbury, Private Bag 4800, Christchurch, New Zealand*
[17] *Dept. of Physics, University of Maryland, College Park, MD 20742, USA*
[18] *Dept. of Physics and Center for Cosmology and Astro-Particle Physics, Ohio State University, Columbus, OH 43210, USA*
[19] *Dept. of Astronomy, Ohio State University, Columbus, OH 43210, USA*
[20] *Dept. of Physics, TU Dortmund University, D-44221 Dortmund, Germany*
[21] *Dept. of Physics, University of Alberta, Edmonton, Alberta, Canada T6G 2G7*
[22] *Dept. of Physics and Astronomy, University of Gent, B-9000 Gent, Belgium*
[23] *Max-Planck-Institut für Kernphysik, D-69177 Heidelberg, Germany*
[24] *Dept. of Physics and Astronomy, University of California, Irvine, CA 92697, USA*
[25] *Laboratory for High Energy Physics, École Polytechnique Fédérale, CH-1015 Lausanne, Switzerland*
[26] *Dept. of Physics and Astronomy, University of Kansas, Lawrence, KS 66045, USA*
[27] *Dept. of Astronomy, University of Wisconsin, Madison, WI 53706, USA*
[28] *Dept. of Physics, University of Wisconsin, Madison, WI 53706, USA*
[29] *Institute of Physics, University of Mainz, Staudinger Weg 7, D-55099 Mainz, Germany*
[30] *Université de Mons, 7000 Mons, Belgium*
[31] *Bartol Research Institute and Department of Physics and Astronomy, University of Delaware, Newark, DE 19716, USA*
[32] *Dept. of Physics, University of Oxford, 1 Keble Road, Oxford OX1 3NP, UK*
[33] *Dept. of Physics, University of Wisconsin, River Falls, WI 54022, USA*
[34] *Oskar Klein Centre and Dept. of Physics, Stockholm University, SE-10691 Stockholm, Sweden*
[35] *Dept. of Astronomy and Astrophysics, Pennsylvania State University, University Park, PA 16802, USA*
[36] *Dept. of Physics, Pennsylvania State University, University Park, PA 16802, USA*
[37] *Dept. of Physics and Astronomy, Uppsala University, Box 516, S-75120 Uppsala, Sweden*
[38] *Dept. of Physics, University of Wuppertal, D-42119 Wuppertal, Germany*
[39] *DESY, D-15735 Zeuthen, Germany*
[a] *now at Dept. of Physics and Astronomy, Rutgers University, Piscataway, NJ 08854, USA*
[b] *now at Physics Department, South Dakota School of Mines and Technology, Rapid City, SD 57701, USA*
[c] *Los Alamos National Laboratory, Los Alamos, NM 87545, USA*
[d] *also Sezione INFN, Dipartimento di Fisica, I-70126, Bari, Italy*
[e] *now at T.U. Munich, 85748 Garching & Friedrich-Alexander Universität Erlangen-Nürnberg, 91058 Erlangen, Germany*
[f] *now at T.U. Munich, 85748 Garching, Germany*
[g] *NASA Goddard Space Flight Center, Greenbelt, MD 20771, USA*

Acknowledgments

We acknowledge the support from the following agencies: U.S. National Science Foundation-Office of Polar Programs, U.S. National Science Foundation-Physics Division, University of Wisconsin Alumni Research Foundation, the Grid Laboratory Of Wisconsin (GLOW) grid infrastructure at the University of Wisconsin - Madison, the Open Science Grid (OSG) grid infrastructure; U.S. Department of Energy, and National Energy Research Scientific Computing Center, the Louisiana Optical Network Initiative (LONI) grid computing resources; National Science and Engineering Research Council of Canada; Swedish Research Council, Swedish Polar Research Secretariat, Swedish National Infrastructure for Computing

(SNIC), and Knut and Alice Wallenberg Foundation, Sweden; German Ministry for Education and Research (BMBF), Deutsche Forschungsgemeinschaft (DFG), Research Department of Plasmas with Complex Interactions (Bochum), Germany; Fund for Scientific Research (FNRS-FWO), FWO Odysseus programme, Flanders Institute to encourage scientific and technological research in industry (IWT), Belgian Federal Science Policy Office (Belspo); University of Oxford, United Kingdom; Marsden Fund, New Zealand; Japan Society for Promotion of Science (JSPS); the Swiss National Science Foundation (SNSF), Switzerland; D. Boersma acknowledges support by the EU Marie Curie IRG Program; A. Groß acknowledges support by the EU Marie Curie OIF Program; J. P. Rodrigues acknowledges support by the Capes Foundation, Ministry of Education of Brazil; A. Schukraft acknowledges the support by the German Telekom Foundation; N. Whitehorn acknowledges support by the NSF Graduate Research Fellowships Program.

32ND INTERNATIONAL COSMIC RAY CONFERENCE, BEIJING 2011

Studies on the unfolding of the atmospheric neutrino spectrum with IceCube 59 using the TRUEE algorithm

THE ICECUBE COLLABORATION[1]
[1]*See special section in these proceedings*

Abstract: The measurement of the atmospheric neutrino energy spectrum provides information about the diffuse neutrino flux from extragalactic sources. A relative increase of the spectrum toward higher energies could be evidence for neutrino producing hadronic processes in the cosmic high energy accelerators, such as active galactic nuclei or gamma ray bursts. IceCube is currently the largest neutrino detector on Earth and is placed in the antarctic ice at the geographic South Pole. IceCube permits the detection of neutrinos with energies beyond 10^6 GeV. Since the acceptance and the resolution of neutrino telescopes suffer from the finite resolution and limited acceptance, a regularized unfolding method is used to extract the energy distribution of neutrinos from the measured observables. For AMANDA, the unfolding was done with the $\mathcal{RUN}$ algorithm. Based on the basic concept of this program and for data analyses in the ROOT frame, a new deconvolution algorithm (TRUEE) has been written and tested. With this new algorithm, studies on the analysis of the atmospheric neutrino spectrum measured with the IceCube 59 string configuration are presented.

Corresponding authors: Natalie Milke[2] (*natalie.milke@udo.edu*), Wolfgang Rhode[2] (*wolfgang.rhode@udo.edu*), Tim Ruhe[2] (*tim.ruhe@udo.edu*)
[2]*Department of physics, TU Dortmund University, D-44221 Dortmund, Germany*

Keywords: IceCube; TRUEE; RUN; regularized unfolding; atmospheric neutrino; energy spectrum

1 Introduction

IceCube is the largest neutrino detector ever built and is located at the geographic South Pole. It consists of 5160 digital optical modules (DOM) arranged along 86 strings forming a three-dimensional grid covering a cubic kilometer in the glacial ice [1]. While traveling through the ice the high energy neutrino-induced muons produce Cherenkov light which can be detected by the DOMs providing directional and energy information of the muon track. One of the main goals of IceCube is the detection of extragalactic neutrinos for understanding of cosmic ray production in cosmic accelerators. Neutrinos from interactions of cosmic rays with the Earth's atmosphere represent a background for the extragalactic neutrinos. Thus, a precise measurement of the atmospheric neutrino flux is important for understanding this background. Since the spectral index of the flux distribution depending on neutrino energy is lower for extragalactic neutrinos (following the spectral behavior of Fermi accelerated cosmic rays $\gamma \sim 2$ [2]) than for atmospheric neutrinos ($\gamma \sim 3.7$) [3], a contribution of extragalactic neutrinos would cause an enhancement of the flux in the high energy region of the spectrum.

The energy of the primary particles is convoluted with the interaction probability and the detector finite resolution and limited acceptance. Therefore the neutrino energy has to be estimated from energy-correlated, measured observables. For this purpose a regularized unfolding algorithm is developed and applied.

In this paper the atmospheric neutrino sample from the measurement with the IceCube 59 (IC 59) string configuration is used. The energy spectrum is unfolded with the new deconvolution algorithm TRUEE.

2 Regularized unfolding

The convolution of the neutrino energy with the interaction probability and detector response gives us the measured observables in the detector and this relation can be expressed as a Fredholm integral equation of the first kind if neglecting background. From discretization a linear matrix equation can be obtained where the measured distribution is a product of the detector response matrix and the neutrino energy distribution. The response matrix is obtained from Monte Carlo (MC) simulation. Thus, an unfolding algorithm needs as input MC-simulated assumed energy distribution with the resulting distributions of measured observables to determine the detector response and the measured observables distributions from data to estimate the neutrino energy flux.

Every unfolding requires an a-priori assumption about some properties of the result realized in a regularization to reduce strong negative correlations between unfolded data points. Here the Tikhonov regularization [5] is used achieving a smooth distribution by minimizing the curvature of the result during the unfolding fit.

3 Unfolding algorithm TRUEE

In AMANDA, the precursor of IceCube, the **R**egularized **UN**folding ($\mathcal{RUN}$) algorithm [6] was used to unfold lepton energy spectra [7]. $\mathcal{RUN}$ was developed in 1984 using the programming language FORTRAN 77. Therefore $\mathcal{RUN}$ is not easy to install and use in combination with modern software. TRUEE - **T**ime-dependent **R**egularized **U**nfolding for **E**conomics and **E**ngineering problems or just **TRUE** **E**nergy is a new software including the $\mathcal{RUN}$-based unfolding algorithm.

One special property of the $\mathcal{RUN}$ algorithm is the parametrization of unfolded distribution using a superposition of cubic basis splines. The spline coefficients are determined from the unfolding and the superposed function is transformed to the final histogram. At the spline overlaping points (knots) the function is continuously differentiable up to the second derivative, so that a Tikhonov regularization with the second derivatives in the smoothing operator can be performed. The user determines the number of splines by defining the number of knots. Regularization is controlled by the number of degrees of freedom, which can be given by the user but can also be suggested by the software. A small number leads to strong regularization.

TRUEE has been developed within the Collaborative Research Centre SFB 823 in Dortmund. Besides the core regularized unfolding from $\mathcal{RUN}$ the new software contains user friendly functions, which make the procedure of an unfolding analysis more comfortable. The functions used in this analysis are explained in the next section using the IC 59 neutrino sample.

4 Unfolding analysis

For this analysis 10 % of the measured data were used. After event selection a sample of 3160 neutrino events measured within the zenith angle range of 88° to 180° with IC 59 is obtained. Thus, most of the events in the sample were caused by neutrinos having traveled through the Earth before undergoing an interaction inside or in the vicinity of IceCube. For 100 % of the data we expect more than 30000 neutrino-induced events and thus higher statistics in the high energy region. Based on a Monte Carlo study the purity of the sample is estimated to be higher than 95 %, therefore the background formed by atmospheric muons is neglected. The sample is obtained using straight precuts followed by an event selection using the multivariate method Random Forest [8] within the framework Rapid Miner [9].

4.1 Selection of observables

As a first step the selection of energy-dependent observables is made. TRUEE automatically produces scatter plots of the sought-after variable and observables and the related profile histograms to check if a correlation is present. The inspection of scatter plots with different observables showed the correlation between primary neutrino energy and the following observables:

- Number of DOMs having a signal
- Number of strings with at least one hit-DOM
- Track length in a certain time window (MPE-Fit_LDirC)

Figure 1 shows the correlation between neutrino energy and number of DOMs.

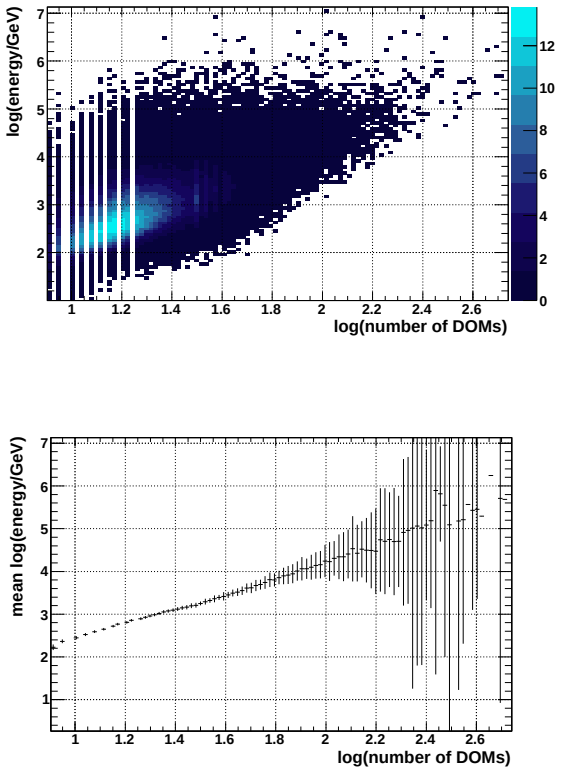

Figure 1: An example of scatter plot and related profile histogram to check the correlation between the energy and the observable (here number of DOMs). An optimal correlation is present in a monotonically changing profile function with small uncertainties.

Since TRUEE is able to use up to three observables at the same time for unfolding, different binnings of the selected observables for the response matrix have been checked. The most suitable binnings could be chosen by inspecting results after running unfolding in the test mode (see Sec. 4.2).

4.2 Test mode

An unfolding algorithm expects input from the user concerning some parameters such as the number of bins for histograms or the degree of regularization. To check which user-defined parameter settings give the optimal unfolding result a test mode is included in TRUEE. In this mode only simulations are used. Since we neglect the atmospheric muon background, the MC sample contains only neutrino events after application of event selection techniques. The energy distribution of simulated neutrino events has been reweighted, so that the generated flux follows the atmospheric neutrino flux predicted by Honda [3] containing a prompt component from Naumov Recombination Quark Parton Model (Naumov RQPM) [4]. The prompt component consists of neutrinos from decays of short-lived mesons containing charm quarks.

An MC sample that is statistically equivalent to the expected experimental data sample is used as a pseudo real data sample for unfolding. Since the real sought-after distribution is known in this case, it can be compared to the unfolded distribution. The optimal parameter settings are chosen with an L-curve approach [10] by examining the tradeoff between regularization strength and fit to the true distribution. For the IC 59 sample the following parameter settings are used for the final unfolding:

- Number of DOMs with 20 bins
- Number of strings with 10 bins
- Track length with 10 bins
- Number of knots 16
- Number of degrees of freedom 5

The unfolded test spectrum is shown in Fig. 2.

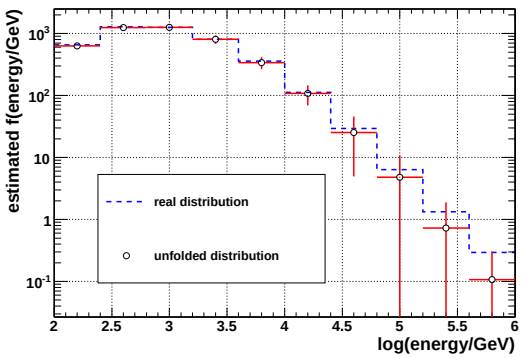

Figure 2: Unfolding of pseudo data compared to the real distribution using test mode. The unfolding does not consider the interaction probability, acceptance or systematic uncertainties.

4.3 Unfolding result

The unfolding procedure with the parameter settings determined in Sec. 4.2 can now be applied to the IC 59 neutrino sample. The generated MC neutrino sample for determination of the detector response contains only simulated events that undergo an interaction within or close to the detector. This procedure is necessary to reduce simulation time and memory. After passing all event selection steps the final sample contains only a fraction of neutrino events. Thus, the unfolded distribution represents only neutrinos which interacted, triggered the detector and passed the event selection (Fig. 3).

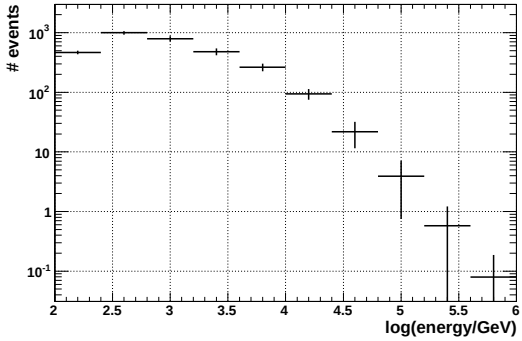

Figure 3: Unfolding of IC 59 data gives the distribution of selected neutrino events depending on energy. The unfolding does not consider the interaction probability, acceptance or systematic uncertainties, yet. Furthermore with the full data sample the number of events per bin will increase by a factor of ten.

To calculate the neutrino flux for all neutrinos within the zenith angle range, the unfolded spectrum has to be divided by the effective area. The effective area is the ratio of observed event rate and incoming flux and depends on the properties of the selected event sample. It includes the muon neutrino cross section, the probability for the muon to be detected and the detector efficiency for muon detection and event reconstruction. The effective area for the current sample is shown in Fig. 4.

The effective area is rising at higher energies due to the increasing cross section of neutrinos and to the higher length of the muon tracks. Therefore the probability to detect and reconstruct such a long track is rising. For the events with vertical upgoing tracks the effective area is decreasing because of the rising probability for absorption of neutrinos by the Earth.

We demonstrate the performance of the unfolding technique by showing an example in Fig. 5 of how an unfolded energy distribution (Fig. 3) can be translated into a neutrino flux spectrum when the effective area (Fig. 4) is known. Additional spectra have been unfolded with the same parameter settings but with different assumptions of the neutrino flux in MC to check the possible bias introduced by the assumption. Shown are results trained with

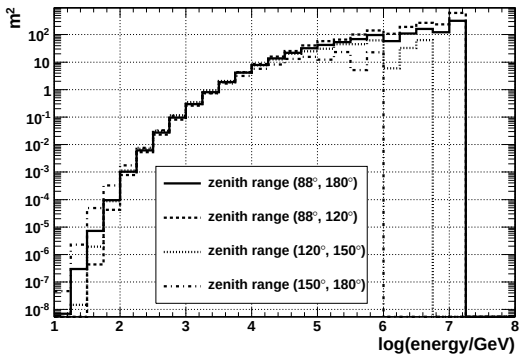

Figure 4: Effective area for the current neutrino sample dependent on neutrino energy. Illustrated are areas for different zenith angle ranges and for the average of the whole zenith range considered in the analysis.

MC weighted to atmospheric (Honda), to atmospheric with prompt (Honda-Naumov) and to atmospheric with prompt and $1.6 \cdot 10^{-8} E^{-2}$ neutrino flux. All three results have only small deviation in the low statistics region, thus the introduced bias is negligible.

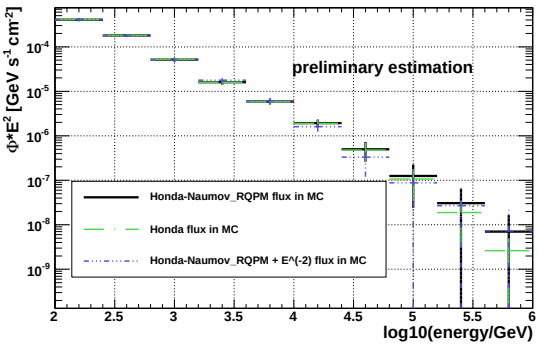

Figure 5: An example of the atmospheric neutrino energy spectrum from 10 % of IC 59 data unfolded with TRUEE. Shown are three unfolding results, using different MC distributions to determine the detector response. The uncertainties take into account statistics and bin-to-bin correlation, determined by the unfolding software. The spectrum is weighted by squared energy for a better illustration.

Since a continuous function is unfolded taking into account event migration between bins, the last bin is estimated to be non-zero even though the statistics of current sample is low.

4.4 Verification of simulation

A function to verify the result was developed in $\mathcal{RUN}$ and was transferred to TRUEE. The user has the possibility to check whether the simulation of all observables agrees with the experimental data and thus verify the unfolding result. After the unfolding, the MC events are reweighted by the unfolded distribution. The MC sample describes the real data now. In this case all observables, not only those which have been used for the unfolding, should match in their distribution the measured data. The observables whose distributions do not match are not correctly simulated. If none of the distributions match, probably the unfolding did not work properly. In this case the user should check if the simulation of the detector response was correct. For the unfolding example shown in this paper the verification showed an agreement between the experimental data and reweighted simulations.

5 Conclusion and outlook

The new unfolding algorithm TRUEE shows a good performance in estimation of an atmospheric neutrino spectrum. The algorithm is able to estimate a steep distribution covering several orders of magnitude and thus is a dedicated tool for astroparticle physics. The analysis is facilitated by additional functions and an easy installation and ease of use of the software.

A new energy region of the atmospheric neutrino flux can be explored with IC 59. The simulation predicts an extension to energies up to 10^6 GeV. The estimation of the neutrino energy spectrum with 10 % of the IC 59 data will be done by unfolding with TRUEE. The subsequent unfolding of the 100 % IC 59 data sample is expected to determine the energy spectrum with more precision in the high energy region due to higher statistics.

6 Acknowledgements

This work is supported by the German Research Foundation DFG (SFB 823/C4 and SFB 876/C3).

References

[1] F. Halzen, S. R. Klein, Rev. Sci. Instrum., 2010, **81**(081101)
[2] E. Fermi, Phys. Rev., 1949, **75**(8): 1169-1174
[3] M. Honda et. al., Phys. Rev. D, 2007, **75**(4): 043006
[4] E. V. Bugaev et. al., Il Nuovo Cimento C, 1989, **12**(1): 41-73
[5] A. N. Tikhonov: 1963, On the solution of improperly posed problems and the method of regularization, Sov. Math. 5
[6] V. Blobel: 1996, The RUN Manual - Regularized Unfolding for High-Energy Physics Experiments, Technical Note TN 361, OPAL
[7] R. Abbasi et. al., Astroparticle Physics, 2010, **34**: 48-58
[8] L. Breiman, Machine Learning, 2001, **45**(1): 5-32
[9] S. Fischer et. al., 2002, Technical Report, Collaborative Research Center 531, University of Dortmund
[10] C. L. Lawson, R. J. Hanson: 1974, Solving Least Squares Problems, Prentice-Hall, Englewood Cliffs, NJ

32ND INTERNATIONAL COSMIC RAY CONFERENCE, BEIJING 2011

Search for atmospheric neutrino induced particle showers with IceCube 40

THE ICECUBE COLLABORATION[1]
[1]*See special section of these proceedings*

Abstract: One of the guaranteed fluxes under study by the IceCube neutrino telescope are neutrinos originating from cosmic ray induced air showers. These neutrinos come from the decay of π and K mesons (the conventional flux) and from the decay of charmed mesons (the prompt flux). Although several flux predictions exist, the electron neutrino flux has been measured only up to GeV energies. At TeV energies, where atmospheric neutrinos are an inevitable source of background events for astrophysical neutrino searches, the prompt flux becomes important and the flux predictions vary greatly. The detection of electromagnetic and hadronic particle showers, which are not only produced by electron neutrinos but which can be found in the final states of charged and neutral current interactions of all neutrino flavours, remains challenging. Given the sensitivity to all neutrino flavours, the good energy resolution that will be possible with fully contained shower events and the possibility to isolate the prompt from the conventional flux, the prospects of this detection channel are very promising. This poster will present an analysis done on a data sample collected with IceCube in its 40 string configuration as it was running from 2008 to 2009. The development of the event selection on a small part of the sample will be discussed.

Corresponding Author: Eike Middell[2] (eike.middell@desy.de)
[2]DESY Zeuthen, Platanenallee 6, 15738 Zeuthen, Germany

Keywords: atmospheric neutrinos, IceCube, particle showers

1 Observing Neutrinos at the South Pole

The possibility to measure or constrain the flux of astrophysical neutrinos could help to solve a number of questions of which one of the most prominent, the question of the origin of cosmic rays, remains unanswered nearly a century after their discovery. Experiments that aim at the detection of these neutrinos must compensate for the small interaction cross sections and the low expected fluxes with increased size. With this year's completion of IceCube [1], the biggest neutrino detector to date, such an experiment is now available. For the experiment a cubic kilometer of glacial ice below the geographical South Pole was instrumented with photomultiplier tubes in order to detect the Cherenkov light of charged secondaries generated in neutrino interactions.

During the last 7 austral summers 86 holes were melted 2.5 km deep into the ice and into each a cable holding 60 so-called Digital Optical Modules (DOMs) has been deployed. The light sensors on 78 of these strings form a grid with a horizontal spacing of 125 m and a vertical distance of 17 m. As the spacing basically determines the energy threshold, the detector center was augmented with the denser DeepCore infill array between 2009 and 2010. The data-taking started already during the construction phase. This work uses data recorded between April 2008 and May 2009 when 40 strings were operational (IceCube 40).

IceCube's main physics goal is the detection of astrophysical neutrinos at energies above 100 GeV. These neutrinos must be isolated from the much larger flux of leptons created in cosmic ray induced air showers [2]. Among these a huge number of muons originating mostly from pion and kaon decays form the biggest part of the background. In the same air showers also atmospheric neutrinos are created [3]. In order to separate them from the astrophysical neutrinos a good understanding of their energy spectrum, flavour ratios and angular distribution will be helpful. This in turn is tightly coupled to our knowledge of the cosmic ray composition and hadronic interactions at energies that are out of reach of accelerator experiments.

The atmospheric neutrino spectrum is expected to consist of two components, the conventional flux from decaying pions and kaons [4, 5] and the prompt neutrinos from decays of short lived charmed mesons [6, 7]. The existing flux predictions for the latter vary widely and current measurements of the muon neutrino flux [8] are not yet able to resolve any prompt from the conventional component (see Fig. 1). Compared to muon neutrinos the flux of atmospheric electron neutrinos is lower and falls with a similar steep power law. Taking advantage of the lower energy threshold of the DeepCore array, IceCube has recently

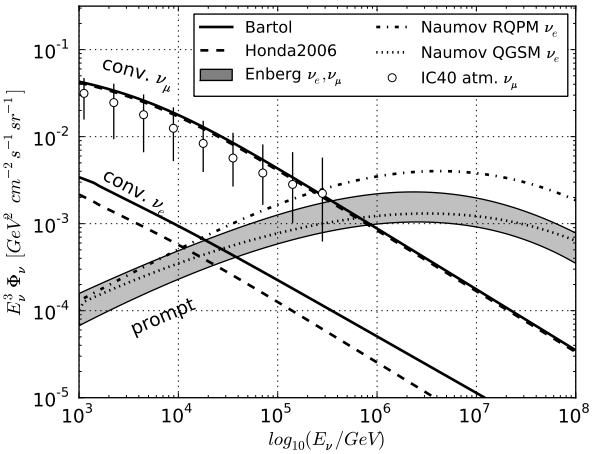

Figure 1: Different flux predictions for atmospheric neutrinos (taken from [4]-[7]) compared to a measurement of the atmospheric ν_μ-flux with IceCube 40 [8].

detected atmospheric neutrino induced showers around a mean energy of $40\,\mathrm{GeV}$ [9]. However, at TeV energies this measurement remains challenging, and only recently an analysis on the same IceCube 40 dataset started to find several promising candidate events [10]. In the energy spectrum of neutrino induced particle showers the prompt component is expected to emerge from the conventional at about 10^5 GeV which is about an order of magnitude lower than for muon neutrinos (see Fig. 1 and [11]). This makes shower events a suitable tool to isolate the prompt component.

2 Neutrino Induced Particle Showers

The events of interest in this study are particle showers emerging from deep-inelastic neutrino nucleon scattering. Particle showers can be found in the final states of charged current (CC) electron and tau neutrino interactions and in all neutral current (NC) interactions. Since IceCube cannot distinguish ν_e and low-energy ν_τ CC interactions from all-flavour NC interactions, analyses tailored to this event signature are effectively sensitive to all neutrino flavours. In NC interactions neutrinos deposit only parts of their energy so they show up as less energetic cascades. This leads to a lower effective area for muon neutrinos.

At TeV energies the particle showers have lengths of a few meters. But due to the large DOM spacing and the scattering of light in the ice showers appear as nearly point-like light sources. This results in spherical hit patterns which at higher energies appear significantly different from the hit patterns of muon tracks.

The separation from the muonic background is mostly impeded by the fact that high energetic muons stochastically undergo catastrophic energy losses in the form of bremsstrahlung showers along the track. Because of the considerable energy deposition these bright electromagnetic showers change the appearance of the track and make them less distinguishable from the searched signal. This has also a connection to the cosmic ray composition because proton air showers produce more often single highly energetic muons than for e.g. iron showers. From the latter often whole bundles of muons reach the detector and traverse the detector nearly in parallel. As the individual muons will have their stochastic energy losses at different positions, the whole bundle appears sufficiently different from a single particle shower and is easier to reject. Extensive simulations performed in the context of similar analyses done on the IceCube 22 dataset confirmed this effect albeit with low statistics. Those muons which passed all cuts were originating from proton air showers [12].

For electromagnetic showers the light yield scales linearly with energy. It has been shown in a Monte Carlo study that for electron neutrino interactions with energies of $10\,\mathrm{TeV}$-$1\,\mathrm{PeV}$ and well contained interaction vertices the energy may be reconstructed with a precision of about $\Delta \log_{10}(E_\nu) = 0.13$ [17].

3 Event Selection

In order to minimize statistical bias a blind analysis is performed. From the 364 days of usable data, 32 days are chosen to develop the event selection. The data was sampled uniformly over the year in order to reflect seasonal variations in the muonic background rate. Secondly, a large background sample of simulated muons from more than 10^{12} air showers were generated. A version of CORSIKA [13] with the Sibyll interaction model was adapted for IceCube and used to simulate the Hörandel polygonato cosmic ray spectrum [14]. Additionally more statistics of protons are currently produced in order to study the impact of composition uncertainties on the background prediction. For the expected signal interactions electron, muon and tau neutrinos were generated with a collaboration-internal simulation package that is based on ANIS [15].

The IceCube 40 detector operated at a trigger rate of about $1300\,\mathrm{Hz}$. An online event selection based on two quickly calculable variables selected events at a rate of $16\,\mathrm{Hz}$. A straight line fit through all hit DOMs at position $\vec{x}_i$ and time t_i yields a parametrization of the form $\vec{x}_i = \vec{x}_0 + \vec{v} \cdot (t_i - t_0)$ where the parameter $|\vec{v}|$ denotes how fast the hit pattern evolves. The second variable uses an analogy to classical mechanics in which it interprets the hit pattern as a rigid body and the recorded amount of light in each DOM as a mass. Spherical hit patterns can then be selected by calculating the eigenvalues of the tensor of inertia and requiring that all three eigenvalues are nearly of the same size. This online filter starts to get efficient above an energy threshold of about $1\,\mathrm{TeV}$ and is optimized for the search for the expected astrophysical E^{-2} flux for which it yields an efficiency of about 73%. For the less energetic atmospheric electron neutrino flux the efficiency is only about 35%.

The selected events were transmitted via satellite to institutes in the North where more elaborate track and vertex likelihood reconstructions can be performed. They provide a sufficient angular resolution for incident muons and with the likelihood value of the vertex reconstruction a quality parameter to select particle showers. Based on the vertex reconstruction also an energy estimator that considers the depth dependent optical properties of the ice [16] is run. Cuts based on these variables reduce the data rate to 2 Hz while keeping about 60% of the atmospheric ν_e signal. According to a predicted atmospheric neutrino flux [5] the sample contains at this point about 1200 ν_e and 10000 ν_μ (CC+NC) events which are still buried below $50 \cdot 10^6$ atmospheric muon events. The effective areas up to this cut level are shown in Fig. 2.

All passing events are fed into a more elaborate likelihood reconstruction [17]. This takes into account the full timing and amplitude information of the recorded light as well as tabulated results of detailed simulations of how light propagates in the ice [18]. For showers this provides estimates for the time and position of the interaction as well as the amount of deposited energy. Also the track reconstruction is repeated with an iterative optimization strategy in order to avoid local minima of the likelihood and to improve the angular resolution for background events [19].

So-called split reconstructions, which split the recorded photons by time into two sets and reconstruct each set individually, provide further information about the event due to the different timing behaviour of tracks and showers. For a track, later hits are downstream along the track while for particle showers they are centered around the vertex but at larger distance.

Based on an argument that shower induced hit patterns should be spherical another cut variable can be constructed. For an imaginary sphere with a given radius and centered at the reconstructed vertex one can calculate the fill ratio N_{hit}/N_{sphere}, where N_{sphere} denotes the number of all DOMs in the sphere and N_{hit} the number of triggered DOMs. This is especially useful to reject events containing several coincident atmospheric muons because the hit patterns of e.g. two coincident but well separated tracks can have many untriggered DOMs in between.

In order to further reduce the muonic background, DOMs at the surface of the instrumented volume are used to veto tracks that appear to enter and traverse the detector. Events for which the first triggered light sensor is located on the outer layer of the detector are rejected. Together with the requirement that the reconstructed vertex is located inside the fiducial volume, this forms a strict containment cut.

Finally those variables that still provide separation power are combined with a machine learning algorithm. In the TMVA framework [20] a boosted decision tree is trained which provides a final cut variable to select particle showers. Current investigations suggest that this event selection is able to remove the remaining background while keeping the prospect to find a few atmospheric neutrinos in the whole sample.

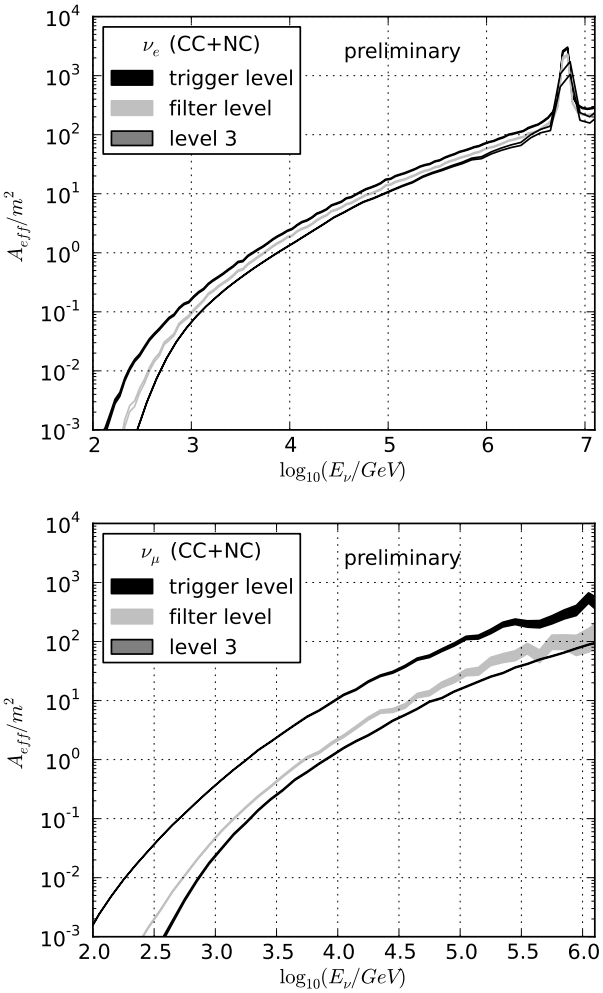

Figure 2: Effective areas for electron and muon neutrinos for the early stages of the analysis. The width of the bands denotes the statistical error. This differs between cut levels because datasets of different size have been used. The peak at 6.3 PeV for electron neutrinos is due to the Glashow resonance. The drop in effective area for muon neutrinos between trigger and online filter level illustrates the effect of tailoring the analysis to neutrino induced particle showers. At the presented cut levels the contribution of muon tracks from charged current interactions is still present. Therefore the effective area is still higher for muon than for electron neutrinos.

However, this statement relies on the Monte Carlo background prediction which has to be scrutinized before unblinding. Accordingly, studies of the systematic uncertainties in the simulated background sample (like for example a lighter cosmic ray composition) are ongoing and will be presented together with the final event selection at the conference.

References

[1] H. Kolanoski, IceCube summary talk, these proceedings.
[2] L. Anchordoqui and T. Montaruli, Ann. Rev. of Nuclear and Particle Science, 2010, **60**:129-162.
[3] T.K. Gaisser and M. Honda, Ann. Rev. of Nuclear and Particle Science, 2002, **52**:153-199.
[4] G.D. Barr *et al.*, Phys. Rev. D, 2004, **70**:023006.
[5] M. Honda *et al.*, Phys. Rev. D, 2007, **75**:043006.
[6] E.V. Bugaev *et al.*, Il Nuovo Cimento, 1989, **12C**:41-73.
[7] R. Enberg *et al.*, Phys. Rev. D, 2008, **78**:043005.
[8] R. Abbasi *et al.*, Phys. Rev. D, 2011, **83**:012001.
[9] IceCube Collaboration, paper 0324, these proceedings.
[10] IceCube Collaboration, paper 0759, these proceedings.
[11] J.F. Beacom and J.Candia, JCAP, 2004, **11**:009.
[12] R. Abbasi *et al.*, arXiv:1101.1692v1,2011
[13] D. Heck *et al.*, Forschungszentrum Karlsruhe, 1998, Report No. FZKA 6019.
[14] J. R. Hörandel, Astropart. Phys., 2003, **19**:193-220.
[15] A. Gazizov, M. Kowalski, Comput.Phys.Commun., 2005, **172**:203-213.
[16] M. Ackermann *et al.*, J.Geophys. Res.,2006 , **111**:D13203
[17] E. Middell, Proc. of the 31st ICRC, 2009, paper 0708
[18] J. Lundberg *et al.*, Nucl. Instrum. Meth. A, 2007, **581**:619-631.
[19] J. Ahrens *et al.*, Nucl.Instrum.Meth.A,2004,**524**:169-194.
[20] A. Hoecker *et al.*, arXiv:physics/0703039, 2007.

Search for a diffuse flux of astrophysical muon neutrinos with the IceCube Detector

THE ICECUBE COLLABORATION[1]
[1] *See special section in these proceedings*

Abstract: The discovery of a cumulative flux of high-energy neutrinos from the sum of all cosmic sources in the Universe is one of the central goals of the IceCube experiment. The experimental signature of isotropically distributed astrophysical sources is an excess of high-energy neutrinos with a characteristic angular distribution over the background of less energetic neutrinos produced when cosmic rays interact with the Earth's atmosphere. Such searches are challenging because of systematic uncertainties in these fluxes and the detector response. The distribution of reconstructed neutrino energies is analyzed using a likelihood aproach that takes into account these uncertainties and simultaneously determines the contribution of an additional diffuse extraterrestrial neutrino component. This analysis is applied to the data measured with the IceCube detector in its 40 and 59-string configurations, covering the period from April 2008 to May 2010. No evidence for an astrophysical neutrino flux was found in the 40-string analysis. The upper limit obtained for the period from April 2008 to May 2009 is $d\Phi/dE \leq 8.9 \cdot 10^{-9}\,\mathrm{GeV}^{-1}\,\mathrm{cm}^{-2}\,\mathrm{s}^{-1}\,\mathrm{sr}^{-1}$ at 90% confidence level in the energy region between 35 TeV and 7 PeV. For the 59-string data from May 2009 to May 2010, an improved analysis technique including the angular distribution in the likelihood approach is presented. The preliminary sensitivity is $d\Phi/dE \leq 7.2 \cdot 10^{-9}\,\mathrm{GeV}^{-1}\,\mathrm{cm}^{-2}\,\mathrm{s}^{-1}\,\mathrm{sr}^{-1}$.

Corresponding authors: Anne Schukraft[2] (*schukraft@physik.rwth-aachen.de*),
Sean Grullon[3] (*sean.grullon@icecube.wisc.edu*), Marius Wallraff[2] (*mwallraff@physik.rwth-aachen.de*)
[2]*III. Physikalisches Institut, RWTH Aachen University, D-52056 Aachen, Germany*
[3]*Dept. of Physics, University of Wisconsin, Madison, WI 53706, USA*

Keywords: IceCube, neutrino astronomy, AGN

1 Introduction

The study of cosmic rays is one of the main aspects of current research in astroparticle physics. Despite all efforts, charged cosmic rays have not yet revealed their sources. A candidate source class is active galactic nuclei, which are believed to accelerate particles up to energies of several EeV by the mechanism of Fermi acceleration, e.g., in the vicinity of their central supermassive black holes. Through hadronic interactions with the surrounding matter and radiation, high-energy neutrinos can be produced. Unlike charged cosmic rays and photons, neutrinos propagate almost unaffected by magnetic fields or intervening matter through the universe. This makes them an ideal messenger particle for astrophysics.
The neutrino telescope IceCube was built at the geographic South Pole with the purpose of detecting neutrinos with energies from several tens of GeV to EeV [1]. It consists of 86 strings each equipped with 60 optical sensors, distributed over an area of roughly $1\,\mathrm{km}^2$ and instrumented in depths from 1.5 to 2.5 km in the Antarctic ice. This huge volume is necessary to compensate for the very low interaction probability of neutrinos with matter. After seven years of construction, the IceCube telescope was completed in December 2010 and is currently the largest detector of its kind in the world.
The detection principle is based on the observation of secondary charged leptons and hadrons produced in interactions of neutrinos in the surrounding ice and rock. These emit Cherenkov light which is detected by IceCube's optical sensors. From the number of photo-electrons and their arrival times, detected by the optical sensors, the neutrino's initial direction and energy are reconstructed. Although no specific neutrino emitting sources have been discovered yet, it is believed that the combined flux of many weak sources distributed all over the sky could be detected with IceCube. This flux would exceed the flux of cosmic ray induced atmospheric neutrinos at high energies and would arrive almost isotropically from all directions. Since it would not be possible to identify individual neutrino sources, this analysis is known as a search for a diffuse neutrino flux.

2 Neutrino Event selection

The first step in the searches for a diffuse astrophysical neutrino flux is to select a sample of neutrino events with high

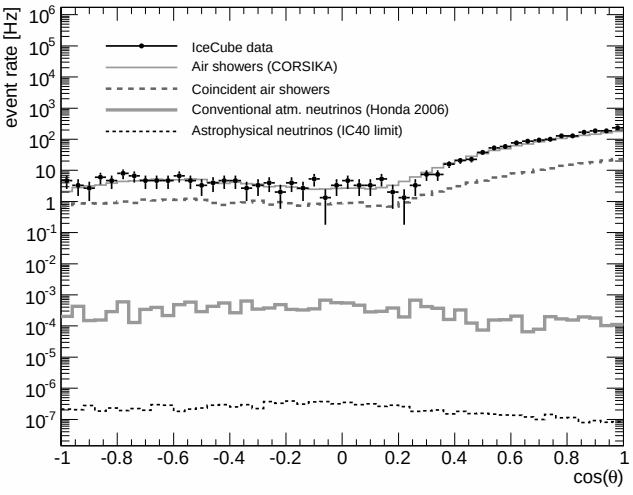

Figure 1: Reconstructed zenith angle distribution of one day of experimental data, and of simulated muons from air showers and neutrino-induced muons with the 59-string configuration at trigger level. The distribution of astrophysical neutrinos is normalized to the 40-string analysis upper limit.

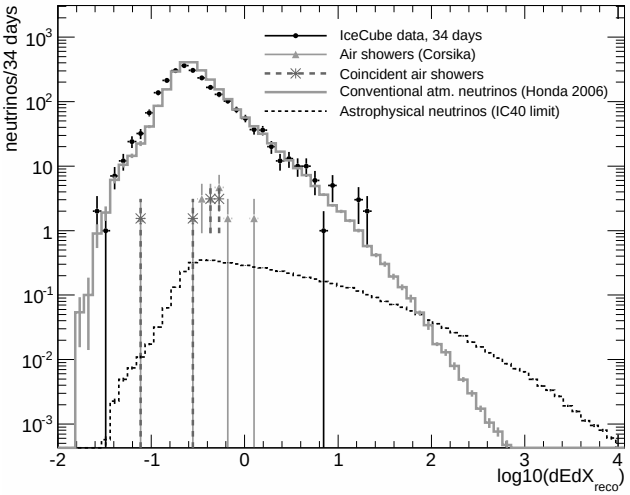

Figure 2: Distribution of the reconstructed muon energy loss for 10% of the 59-string data after neutrino selection.

purity. This contribution presents two searches for a diffuse neutrino flux with data from two consecutive years during the construction of IceCube. Both analyses focus on the selection of high-energy secondary muon tracks. Data was taken from April 2008 to May 2009 in the 40-string configuration and from May 2009 to May 2010 with 59 deployed strings. The event selections and analysis techniques are very similar. The analysis of the 59-string sample has not been finalized.

The reconstructed zenith angle distribution of detected events is shown in Fig. 1. The dominant background in this analysis are muons from cosmic-ray air showers. At trigger level, they outnumber the detected neutrino-induced muons by several orders of magnitude. In contrast to neutrinos, muons are easily absorbed by the Earth. Therefore, muons produced in the atmosphere enter the detector from above and are primarily reconstructed as downward going tracks, while muons originating from neutrinos interacting with the matter surrounding the detector come from all directions.

To reject a large amount of air shower background the analysis is restricted to upward reconstructed muon tracks. The remaining background is misreconstructed air-shower-induced muon tracks, containing a large fraction of muons arriving from coincident but independent air showers. For the further selection, an algorithm searches for patterns separated in space and time in the ensemble of recorded light-sensor pulses. This allows rejection of coincident events as well as tracks associated with random noise hits.

For the selection of a high-purity upward-going neutrino sample, the remaining data is reduced by a series of quality-criteria applied to reconstructed variables like the directional estimate of the reconstruction. They are described in detail in [5]. The final event sample consist of 12877 neutrino candidate events for the 40-string configuration and about 25000 expected events for the 59-string configuration after finalization of the analysis. Based on Monte Carlo simulation, the expected contamination of remaining background events is less than 1%.

Figure 2 shows the distribution of the reconstructed average energy losses for the selected muon tracks along their path in the detector. The experimental data is largely consistent with the expectation from atmospheric neutrinos. Most interesting for this analysis are events with high energy depositions.

3 Analysis method

The irreducible background for astrophysical neutrino searches consists of conventional atmospheric neutrinos. These neutrinos are produced in the decay of pions and kaons in cosmic-ray air showers in the Earth's atmosphere. They are described by an energy spectrum following a power law of about $d\Phi/dE \propto E^{-3.7}$ and by a characteristic zenith angle distribution related to the meson's path through the atmosphere. Another – not yet observed – type of atmospheric background are so called prompt neutrinos. Prompt neutrinos originate from the decay of heavier mesons, typically containing a charm quark[3]. They are produced at a higher cosmic-ray energy threshold and because of their comparably short lifetimes their energy distribution is predicted to follow a harder energy spectrum of $d\Phi/dE \propto E^{-2.7}$ with an almost isotropic angular distribution.

The aim of this analysis is to identify a possible astrophysical component in the neutrino sample. An astrophysical flux can be distinguished from a conventional atmospheric

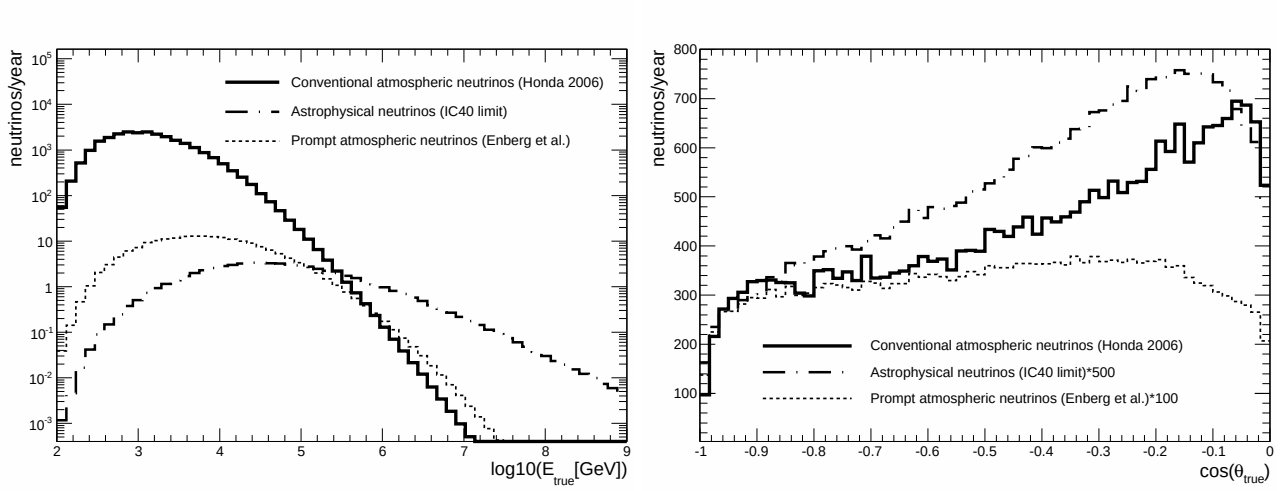

Figure 3: Expected energy (left) and zenith (right) distribution for detected conventional atmospheric neutrinos, prompt atmospheric neutrinos and astrophysical neutrinos in the IceCube detector with 59 strings. Left: The astrophysical neutrino flux is normalized to the upper limit (90% CL) of the 40-string analysis presented here. Right: The astrophysical and prompt fluxes have been renormalized for better visualization.

flux by its harder energy spectrum. Assuming shock acceleration in the extragalactic sources, an astrophysical neutrino flux would follow a $d\Phi/dE \propto E^{-2.0}$ power law (see Fig. 3). With the presumption of isotropically distributed sources over the whole sky, the arrival directions of these neutrinos would be isotropic. Their energy spectrum being harder than that of conventional atmospheric neutrinos, prompt neutrinos are an important background in a search for a diffuse flux.

Relative to the 40-string analysis[5], the ongoing 59-string analysis improves the sensitivity to an astrophysical flux by considering directional information in addition to energy. Figure 3 shows the expected zenith angle distribution of arrival directions when considering the energy-dependent absorption in the Earth, the angular detector acceptance and event selection efficiency. The significant differences in angular distribution for neutrinos of different origin adds separation power between the three components.

A likelihood method is applied to the experimental data to fit for the contributions of conventional atmospheric neutrinos, prompt atmospheric neutrinos and astrophysical neutrinos. In the 40-string analysis, the corresponding one-dimensional probability density functions (pdf) of the reconstructed energy are used to determine the probability for an astrophysical and prompt component. For the 59-string analysis, two-dimensional pdfs of reconstructed energy loss and zenith angle are used to account for both parameters and their correlation. Systematic uncertainties are taken into account by incorporating nuisance parameters in the likelihood function. These uncertainties are discussed in the next section.

The test statistic is a profile likelihood based on a likelihood ratio of the best fit of all physics and nuisance parameters to the experimental data compared to a fit of only the nuisance parameters for each point in the physics parameter space. Confidence regions are constructed according to the Feldmann & Cousins approach by generating a large number of random experiments based on Monte Carlo simulations[7]. In order to estimate the sensitivity of the analysis to a signal of diffuse astrophysical neutrinos, random experiments assuming the zero-signal hypothesis are generated.

4 Systematic uncertainties

A challenge in the search for a diffuse neutrino flux is the treatment of systematic uncertainties. Unlike other analyses of IceCube data, the background cannot be estimated from an off-source region in the experimental data. Therefore, the background estimation relies on a full-chain detector simulation. Inputs are, amongst others, air showers simulated with CORSIKA [4] and atmospheric neutrinos based on [2, 3]. More details can be found in [5, 6].

Main uncertainties at high energies are the conventional and prompt atmospheric neutrino flux predictions, the calculated neutrino cross sections and in particular the modeling of the detector response. Examples for the latter are the optical properties of the Antarctic glacial ice and the absolute efficiency of the optical sensors. The influence of these uncertainties on the final result is determined by studying simulations with different settings of these parameters. Some uncertainties, such as in the spectral index of atmospheric neutrinos, are taken into account with nuisance parameters in the likelihood fit. Additional information on the sytematic uncertainties can be found in [5, 6].

One possibly significant uncertainty not taken into account in the 40-string analysis is the effect of the knee in the cosmic-ray spectrum on the energy spectrum of conventional atmospheric neutrinos. This leads to an expected

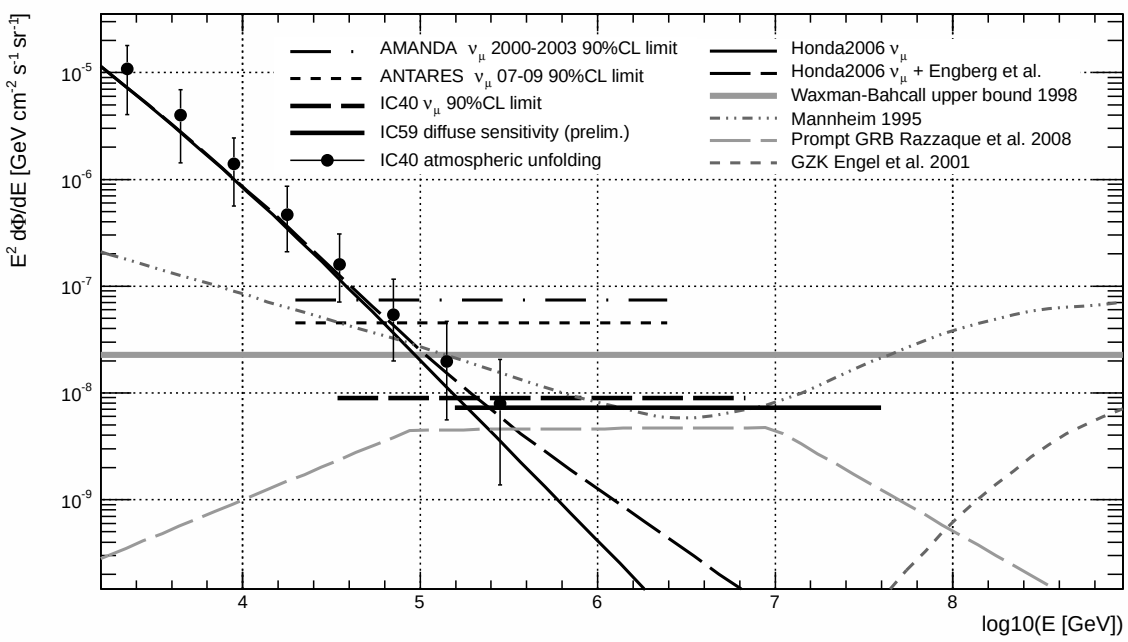

Figure 4: Limits and predictions for diffuse muon neutrino fluxes. The thin black lines show the expected flux for atmospheric neutrinos without and with an additional prompt component together with the unfolded atmospheric neutrino spectrum by IceCube[6]. The black horizontal lines represent 90%-confidence-level upper limits from different experiments [8, 9, 5]. The gray curves represent theoretical flux predictions for AGN models [11], gamma ray bursts [12] and GZK neutrinos [13]. The thick gray line shows the Waxman-Bahcall upper bound [10].

steepening of the neutrino spectrum above several tens of TeV, which is within the energy range relevant for this analysis but which has so far not been included in our simulations. The systematic uncertainties related to such a neutrino knee will be incorporated into the 59-string analysis using parameterizations of the measured cosmic-ray spectra.

5 Results

The result of the 40-string diffuse neutrino search has been published in [5]. The measured energy distribution is consistent with the expectation from conventional atmospheric neutrinos only. No prompt atmospheric nor astrophysical flux component was found. A small underfluctuation relative to the expectation was observed in the high-energy tail. This results in an upper limit on an astrophysical neutrino flux $d\Phi/dE \propto E^{-2.0}$ of $d\Phi/dE \leq 8.9{\cdot}10^{-9}\,\mathrm{GeV}^{-1}\,\mathrm{cm}^{-2}\,\mathrm{s}^{-1}\,\mathrm{sr}^{-1}$ integrated over the energy range between 35 TeV and 6.9 PeV with 90% confidence. This is currently the most constraining limit on a diffuse astrophysical neutrino flux and about a factor of two below the Waxman-Bahcall upper bound for an astrophysical neutrino flux [10]. At the same confidence level, a prompt atmospheric flux at 70% of the most probable flux predicted by Enberg et al.[3] was ruled out.

The higher statistics of the neutrino sample from the larger 59-string detector improves the sensitivity to astrophysical fluxes by about 35% compared to the 40-string analysis. The additional gain from using directional information is about 10% and results in a sensitivity of $d\Phi/dE \leq 7.2{\cdot}10^{-9}\,\mathrm{GeV}^{-1}\,\mathrm{cm}^{-2}\,\mathrm{s}^{-1}\,\mathrm{sr}^{-1}$ (Fig. 4). A further gain of roughly 10% in sensitivity for astrophysical fluxes is expected when taking into account the effect of the knee in the cosmic-ray spectrum.

References

[1] A. Achterberg et al., Astropart. Physics, 2006, **26** (155)
[2] M. Honda et al., Phys. Rev. D, 2007, **75** (043006)
[3] R. Enberg et al., Phys. Rev. D, 2008, **78** (043005)
[4] D. Heck et al., CORSIKA: A monte carlo code to simulate extensive air showers, Tech. Rep. FZKA, 1998
[5] R. Abbasi et al., arXiv:1104.5187v1, 2011 (submitted)
[6] R. Abbasi et al., Phys. Rev. D, 2011, **83** (012001)
[7] G. Feldman and R. Cousins, Phys. Rev. D., 1998, **57** (3873)
[8] A. Achterberg et al., Phys. Rev. D, 2007, **76** (042008)
[9] S. Biagi, Search for a diffuse flux of muon neutrinos with the antares telescope, Conference presentation at NEUTRINO 2010 Athens, Greece (2010)
[10] E. Waxman and J. Bahcall, Phys. Rev. D., 1998, **59** (023002)
[11] K. Mannheim, Astropart. Phys, 1995, **3** (295)
[12] S. Razzaque and P. Meszaros, Phys. Rev. D, 2003, **68** (083001)
[13] R. Engel, D. Seckel, and T. Stanev, Phys. Rev. D, 2001, **64** (093010)

32ND INTERNATIONAL COSMIC RAY CONFERENCE, BEIJING 2011

Search for astrophysical neutrino-induced cascades using IceCube-40

THE ICECUBE COLLABORATION[1]
[1]*See special section in these proceedings*

Abstract: IceCube is the first cubic-kilometre scale neutrino observatory dedicated to detecting astrophysical neutrinos. A large contribution to the expected neutrino signal is from electromagnetic and hadronic showers (cascades) initiated by charged current ν_e interactions, and neutral current ν_e, ν_μ and ν_τ interactions. Cascade energy is reconstructed with better resolution than muons, and the atmospheric background is lower. The energy spectrum of astrophysical neutrinos is expected to be harder than that of atmospheric neutrinos, so an astrophysical neutrino signal could be observable as a break in the cascade energy spectrum.

Cascades are difficult to detect due to a large background coming from atmospheric muons and muon bundles, many orders of magnitude larger than the cascade signal. Large statistics, advanced reconstruction methods and machine learning techniques are required to isolate cascade events within the data. There is growing evidence for neutrino-induced cascade events in IceCube in several analyses that were carried out using data from April 2008 to May 2009, when 40 IceCube strings were operational. This is the largest instrumented volume, and yields the most sensitive search for a diffuse flux of astrophysical neutrinos using cascades to date.

Two of the IceCube-40 analyses are described in these proceedings. The high energy analysis measures four background events, and sets a 90% confidence level limit for all flavour astrophysical neutrino flux of 9.5×10^{-8} $\mathrm{GeVsr^{-1}s^{-1}cm^{-2}}$ over the energy range 89 TeV to 21 PeV. The mid energy analysis observes 14 cascade candidate events. The background to these events is under investigation. Three of the observed events have reconstructed energies above 100 TeV.

Corresponding authors: Stephanie Hickford[2] (*stephanie.hickford@pg.canterbury.ac.nz*), Sebastian Panknin[3] (*sebastian.panknin@icecube.wisc.edu*)
[2]*Department of Physics and Astronomy, University of Canterbury. Private Bag 4800, Christchurch, New Zealand*
[3]*Institut für Physik, Humboldt-Universität zu Berlin, Newtonstr. 15, 12489 Berlin*

Keywords: IceCube; neutrinos; cascades

1 Introduction

High energy neutrino production is predicted to occur in regions of the universe containing astrophysical objects that emit large amounts of energy [1]. The same regions are predicted to emit the highest energy cosmic rays, whose origins are yet unknown. These are dense regions where large gravitational forces generate relativistic jets, accelerating charged particles. This is associated with objects such as supernovae, gamma ray bursts, and active galactic nuclei. High energy neutrinos originating from these objects may be observed as a diffuse flux by detectors such as IceCube.

A large proportion of the expected diffuse flux which interacts with nucleons in the detector results in particle showers (cascades). IceCube is capable of detecting cascades produced from all flavours of neutrinos. Cascade energy is reconstructed with better resolution than that from track-like particles such as muons, since cascades are fully contained in the detector. Also cascades have lower atmospheric neutrino background flux. The astrophysical flux has a harder energy spectrum than that of atmospheric neutrinos, which makes diffuse searches a promising route for observing a break in the energy spectrum of neutrinos from astrophysical sources. A previous cascade analysis in IceCube [2] has shown progress towards a detection of atmospheric neutrinos, and set a limit of 3.6×10^{-7} $\mathrm{GeVsr^{-1}s^{-1}cm^{-2}}$ on astrophysical neutrinos (assuming a 1:1:1 flavour ratio) for the energy range 24 TeV to 6.6 PeV, using the 22 string IceCube detector. There are several cascade analyses using the larger 40 string IceCube detector: two low energy analyses described in other proceedings at this conference [3, 4], and the two high energy analyses described here. The goal of these high energy analyses is to search for astrophysical neutrino-induced cascades.

2 IceCube-40 Data

IceCube is a Cherenkov neutrino detector located at the South Pole. The detector is comprised of Digital Optical Modules (DOMs) [5] situated on strings deployed deep

in the Antarctic ice. The DOMs house photomultiplier tubes (PMTs) [6], along with data acquisition software, in a pressure vessel. There are 60 DOMs on each string which detect Cherenkov light from charged particles traveling through the ice. The analyses described here uses data from when the detector was still under construction, when 40 strings were deployed and acquiring data. Figure 1 shows the IceCube-40 detector configuration.

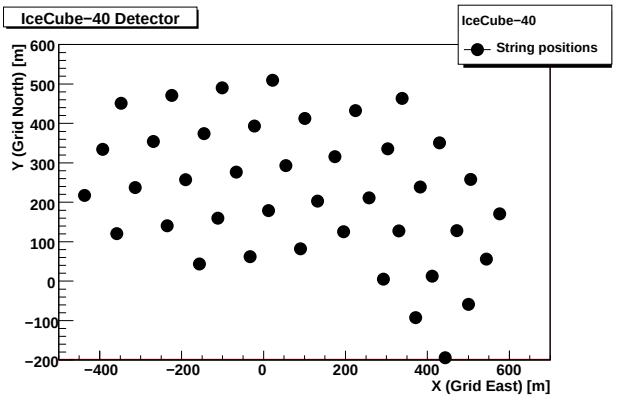

Figure 1: IceCube-40 detector configuration.

The IceCube-40 detector was operational from 6^{th} April 2008 to 20^{th} May 2009. During physics runs all event information was sent from DOMs to the surface for processing if the trigger condition was met. The trigger condition requires 8 DOMs to be hit within 5000 ns. The IceCube-40 physics dataset contains 374 days of data.

3 Analysis

The analyses presented here [10, 11] search for an E^{-2} neutrino flux within the IceCube-40 dataset. These searches use cuts on reconstructed event variables, reducing the background from atmospheric muons to isolate cascade events originating from astrophysical sources.

Neutrino interactions of all flavours were simulated to predict the expected signal. This was done using Monte Carlo simulations with an energy spectrum of E^{-1}. These simulated events were then re-weighted for atmospheric and astrophysical neutrino spectra. The atmospheric re-weighting uses the Bartol model [7] for the conventional neutrino flux, and the Sarcevic model [8] for the prompt neutrino flux. The astrophysical re-weighting uses an E^{-2} spectrum.

The dominant background to these analyses comes from atmospheric muons, simulated using Monte Carlo techniques with CORSIKA [9]. The simulation was used to train machine learning algorithms to develop cuts to separate signal from background.

3.1 Filter Levels of Mid Energy Analysis

The first level of filtering is run online at the pole in order to reduce the data volume to an acceptable level for transfer via satellite. The pole filter for the cascade stream during IceCube-40 consisted of two cuts placed on reconstructed variables. The first variable is a fit to the hit timing, and is placed to reject track-like events with a high velocity, and keep cascade-like events with low velocities. The second variable uses the hit topology of the event defined by Tensor of Inertia eigenvalues. The cut rejects elongated track-like events, and keeps highly spherical cascade-like events by cutting on the ratio of lowest eigenvalue to the sum of the three. After the data is transferred, level 2 processing is run, which consists of further reconstructions used in higher level filtering.

The level 3 filter reduces the background further in order to run more advanced reconstruction algorithms. This filter was applied only to events with a reconstructed cascade energy below 10 TeV, where the background is most dominant. The first cut variable is the reconstructed zenith direction assuming a plane-wave track topology. Events coming from above the horizon ($\theta_{\mathrm{z}} < 80^{\circ}$) are removed. The second cut variable is the reduced log likelihood. This variable is derived from the likelihood that an event is a cascade, based on the hit pattern in the detector. Events less likely to be cascades are removed.

The level 4 filter reduces the background further to run more sophisticated reconstructions with better variable resolutions. There are three cuts at this level. The first cut is on the reconstructed energy, placed at 2.5 TeV. The two further cuts at this level are on Spatial Distance and Fill Ratio reconstructions. The Spatial Distance cut splits the event into two parts based on the timing of hits, with the vertex position from each half reconstructed separately. If the event is a spherical cascade-like event the two vertex positions are expected to be at the same location in the detector. If the event is an elongated track-like event the two vertex positions will be located far apart. This cut requires that the two reconstructed vertex positions be within 40 m of each other. The Fill Ratio cut defines a sphere based on the radius from the mean position of hit DOMs around the reconstructed vertex of an event, and looks at the ratio of DOMs hit within this sphere over the total number of DOMs. If the event is a spherical cascade-like event the fill ratio is expected to be close to one. If the event is an elongated track-like event the fill ratio will be much less than one. This cut requires at least 40% of DOMs within the sphere to have hits.

The level 5 filter consists of containment cuts. These cuts are necessary as most of the remaining background events are located at the edges of the detector. The first containment cut is on the reconstructed vertex position. This cut requires that the vertex of the event be more than 50 m inside the top and bottom of the detector, and inside the outer ring of strings (string containment). The second containment cut is on the charge received by each DOM. This cut requires that the DOM with the largest charge be located on an inner string (DOM charge containment). The effect of these containment cuts is shown in Figure 2. After these cuts are applied, background and signal simulation are fed

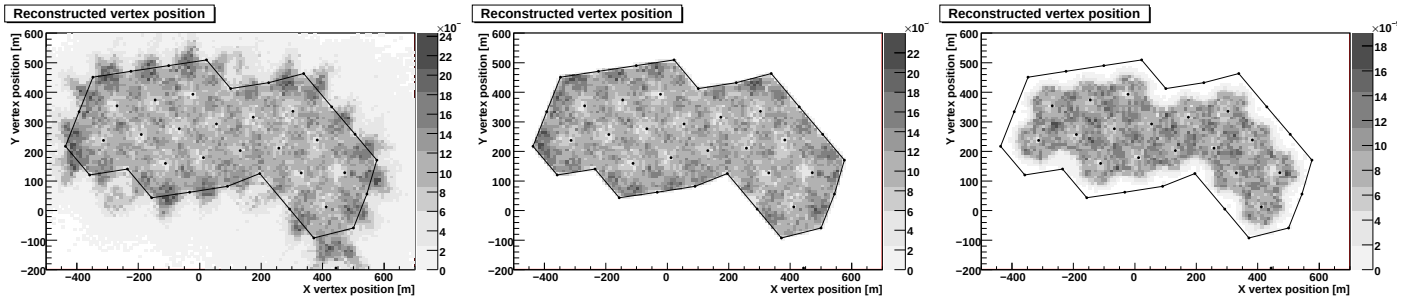

Figure 2: IceCube-40 detector in xy coordinates, black dots are the string positions. Each figure shows the reconstructed vertex for simulated E^{-2} signal. **a)** Before containment, **b)** after string containment, **c)** after DOM charge containment.

into a machine learning algorithm. Multivariate analysis (TMVA) [12] is used, which assigns a boosted decision tree (BDT) response score to each event. This BDT response has a strong separation power. The variables used for machine learning are:

- **Z vertex position** Reconstructed event depth.
- **Zenith track direction** Reconstructed zenith angle.
- **Log likelihood** Likelihood event arises from a muon.
- **Linefit velocity** Particle speed to create hit pattern.
- **Eigenvalue ratio** Topology of event.
- **Fill ratio** Ratio of DOMs hit in sphere around vertex.
- **Time split** Difference in time of two halves of event.
- **Containment** Event distance from detector centre.

The level 6 filter is the final level of cuts. There are two cuts at this level: the BDT response from multivariate analysis, and the reconstructed energy. These cut values are optimised using the Feldman-Cousins [13] method. The BDT response cut is 0.2, and the energy cut is 25 TeV.

3.2 Filter Levels of High Energy Analysis

This analysis was designed to quickly reach a result, and thus accepted a higher energy threshold [11]. It follows the mid energy analysis to level 3, then a BDT was trained using ten variables connected to shape, fit quality and position of the event. Each variable has a correlation of less than 30% to reconstructed energy, so BDT score and energy can be used as quasi-independent variables to suppress background in the final level. These cuts were optimised for sensitivity [14], based only on simulation. The background is very sensitive to cosmic ray composition, ice and detector properties. In addition, limited statistics for rare events made the background prediction fragile. The atmospheric muon prediction is $0.72 \pm 0.28(\mathrm{stat}) \pm^{1.54}_{0.49} (\mathrm{sys})$ events, with a large systematic error that is based on a detailed comparison of simulation with data. The systematic uncertainty will be reduced with future simulation. The signal prediction for an all flavor E^{-2} flux of 10^{-7} $\mathrm{GeVsr}^{-1}\mathrm{s}^{-1}\mathrm{cm}^{-2}$ is $7.93 \pm 0.13(\mathrm{stat}) \pm 1.47(\mathrm{sys})$ events (assuming a flavor ratio of 1:1:1).

4 Results

4.1 High Energy Analysis

In the high energy analysis four events were found. After careful inspection, all events look similar to background from atmospheric muons. Due to the systematic error this result is compatible with a null hypothesis. A limit at 90% confidence level on the astrophysical neutrino flux was set using the method of Rolke et. al. [15]:

$$\Phi_{\mathrm{lim}}\mathrm{E}^{-2} \leq 9.5 \times 10^{-8}\mathrm{GeVsr}^{-1}\mathrm{s}^{-1}\mathrm{cm}^{2}. \qquad (1)$$

The energy range containing 90% of the signal is 89 TeV to 21 PeV. A comparison with model predictions and other analyses limits is shown in Figure 3.

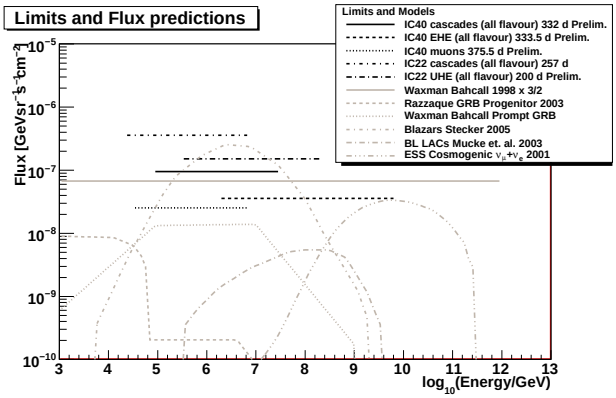

Figure 3: Limits and flux predictions for an all flavor diffuse flux. Black lines indicate limits, this high energy analysis is the solid line. The current best limit is given by the IceCube-40 diffuse search using muon neutrinos [16]. Theoretical models are thin grey lines.

4.2 Mid Energy Analysis

In the mid energy analysis a total of 14 events were observed. Of these, four events contained early hits, with timing from before the cascade. This could indicate a background event due to an atmospheric muon interaction, a muon neutrino interaction, or muon production within the

cascade. The background prediction is under investigation. The remaining events contain no evidence of early hits, and after visual inspection appear to be high quality cascade candidate events, including three that have reconstructed energies above 100 TeV.

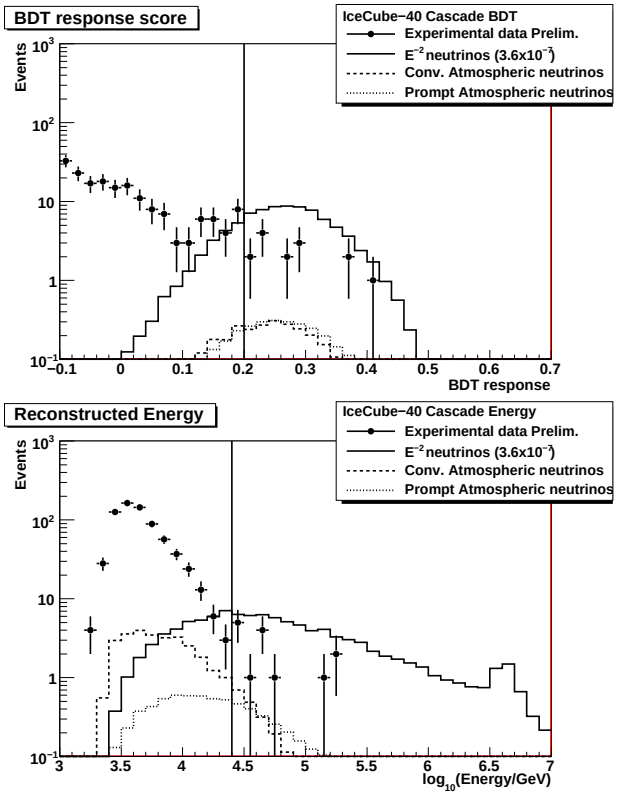

Figure 4: Distributions with final cut values shown by the vertical lines. **a)** BDT response, **b)** Energy spectrum.

Figure 4 shows the BDT response and energy spectrum distributions. Experimental data, E^{-2} signal prediction, and expectation from atmospheric cascades are shown. E^{-2} signal assumes a flux of $3.6\times10^{-7}\ \mathrm{GeV sr^{-1} s^{-1} cm^{-2}}$, the limit set by previous IceCube-22 cascade analyses [2]. The vertical line on these distributions indicates the cut value of 0.2 for BDT response and 25 TeV for reconstructed energy. On the right hand side of these cut values are the 14 events, which lie above the prediction from atmospheric cascades. Figure 5 shows a cascade event in IceCube-40 observed by the mid energy analyses. This event has a BDT response of 0.236, and a reconstructed energy of 144 TeV.

5 Summary

Results of the searches for an E^{-2} astrophysical neutrino flux with IceCube-40 are presented. The high energy analysis observed four background events and set a limit of $9.5\times10^{-8}\ \mathrm{GeV sr^{-1} s^{-1} cm^{-2}}$. The mid energy analysis observed 14 events. The majority of these events appear to be good cascade candidates, while four contain evidence of muon tracks. These four events could be background

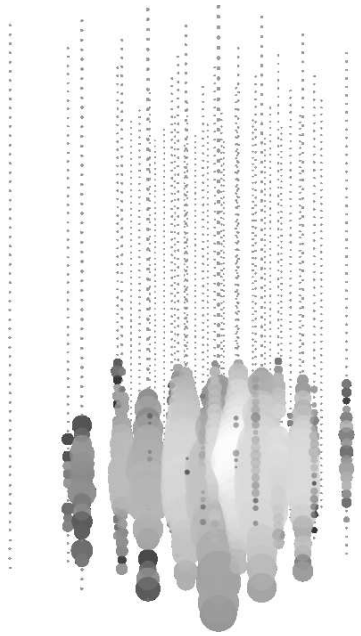

Figure 5: Cascade event in IceCube-40. Small dots are position of DOMs, circles show light received, where size indicates number of photons.

events, or muons from muon neutrino interaction or within the cascade. Using atmospheric neutrino models Bartol and Sarcevic, 1.8 conventional events and 2.1 prompt events are predicted from atmospheric neutrinos. The events are currently being investigated by performing more extensive background simulations.

References

[1] F. Halzen, AIP Conf. Proc., 2009, **1182**: 14-21
[2] R. Abbasi et. al., ArXiv e-prints 1101.1692, Jan 2011
[3] IceCube Collaboration, paper 1097, these proceedings
[4] IceCube Collaboration, paper 0324, these proceedings
[5] R. Abbasi et. al., Nucl. Instrum. Meth., 2009, **A601**: 294-316
[6] R. Abbasi et. al., Nucl. Instrum. Meth., 2010, **A618**: 139-152
[7] G.D. Barr, T.K. Gaisser, P. Lipari, S. Robbins, T. Stanev, Phys. Rev., 2004, **D70**: 023006
[8] R. Enberg, M.H. Reno, I. Sarcevic, Phys. Rev., 2008, **D78**: 043005
[9] D. Heck et. al., FZKA, 1998, 6019
[10] S. Hickford, PhD Thesis, 2011 (in preparation)
[11] S. Panknin, PhD Thesis, 2011 (in preparation)
[12] A. Hocker et. al., PoS ACAT 2007, 040
[13] G.J. Feldman and R.D. Cousins, Phys. Rev., 1998, **D57**: 3873-3889
[14] G.C. Hill and K. Rawlins, Astropart. Phys., 2003, **19**: 393-402
[15] W.A. Rolke, A.M. Lopez, J. Conrad, Nucl. Instrum. Meth., 2005 **A551**: 493-503
[16] R. Abbasi et. al., ArXiv e-prints 1104.5187, Apr 2011

32ND INTERNATIONAL COSMIC RAY CONFERENCE, BEIJING 2011

The baseline capability of the cosmogenic neutrino search with IceCube

THE ICECUBE COLLABORATION[1]
[1]*See the special section in these proceedings*

Abstract: We present the expected baseline sensitivity of the IceCube detector to cosmogenic neutrinos produced through the GZK process. Data from the partially completed IceCube detector have previously been searched for such highly energetic ($\geq 10^6$ GeV) neutrinos. With the completion of the detector in December 2010 and the full operation having started in May 2011, IceCube's sensitivity to these neutrinos is significantly improved from previous studies. We calculate the expected sensitivity in the search of cosmogenic (GZK) neutrinos using a Monte Carlo simulation of the completed IceCube detector and the selection criteria developed in the previous analysis. The sensitivity for a diffuse flux of cosmic neutrinos with an E^{-2} spectrum in the central 90% energy range 300 TeV to 2 EeV is expected to be at a level of $E^2\phi_{\nu_e+\nu_\mu+\nu_\tau} \leq 1.3 \times 10^{-8}$ GeVcm^{-2} sec^{-1}sr^{-1} with one year of operation. The corresponding differential sensitivity is also presented.

Corresponding author: Aya Ishihara[2] (*aya@hepburn.s.chiba-u.ac.jp*)
[2]*Chiba University, Yayoi-cho 1-33, Inage-ku, Chiba, Chiba, 26-0045 Japan*

Keywords: IceCube, cosmogenic neutrinos, GZK mechanism

1 Cosmogenic neutrinos with IceCube

Cosmogenic neutrinos are produced in the interactions of the highest energy cosmic-rays with the cosmic-microwave background (CMB) photons (the GZK process [1, 2]) and subsequent charged pion decays [3]. These cosmogenic (GZK) neutrinos are one of the most promising messengers from the high energy, distant universe beyond PeV energies. They may provide us with direct evidence of the highest energy cosmic ray sources unlike the other messengers, such as gamma-rays and cosmic-rays, which experience interactions with the CMB and/or galactic and extra-galactic magnetic fields.

IceCube is a cubic kilometer scale deep underground Cherenkov neutrino detector at the South Pole. The IceCube detector construction was completed in December 2010. The IceCube array [4] comprises 5160 optical sensors on 86 cables, called strings, over a 1 km^3 fiducial volume of ice at a depth of 1450 m $\sim$ 2450 m. In 2008-2009, 40 out of 86 cables were deployed and taking data with an approximate fiducial volume of 0.5 km^3. Results from the cosmogenic neutrino search with the half-completed configuration of IceCube [5] generated the best published limit to date on the neutrino fluxes above 1 PeV and up to 10 EeV.

In this proceeding, we present the expected sensitivity of the completed IceCube detector to cosmogenic neutrino fluxes calculated using a Monte Carlo simulation. The signal discrimination methods are based on the selection criteria utilized in the 2008-2009 data analysis with the partially instrumented 40-string detector [5].

In the energy region above 1 PeV, the primary variable used to discriminate signal from background is the energy of

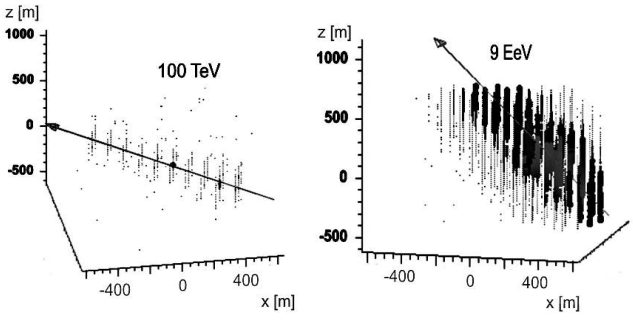

Figure 1: Simulated single muon events in IceCube. Left panel shows a 100 TeV muon track representing the conventional event while the right panel indicates a 9 EeV muon EHE event. Circles denote optical sensors with more than one photo-electron signal recorded. The size of the circles represents the number of photo-electrons. Axes are distances in meters from the center of the IceCube detector array.

the particles. This is because the conventional atmospheric neutrino and muon background spectra are proportional to $\mathrm{E}^{-3.7}$ or steeper, while signal spectra follow $\mathrm{E}^{-1} \sim \mathrm{E}^{-2}$ in the energy region considered. Since the amount of energy deposited in the form of Cherenkov photons by the neutrino-induced charged particles in the detector is highly correlated with their energy, the extremely-high energy neutrino signal stands out against the atmospheric muon and neutrino background because of the much higher light deposition. The total number of photo-electrons (NPE) recorded in an event is used as the main distinctive feature to separate signal from background. Figure 1 illustrates the difference in the energy deposition in the IceCube detector from a background-like 100 TeV muon and a signal-like 9 EeV muon.

2 Event selection

The primary background in this analysis is muon bundles made up of large numbers of muons produced by high energy cosmic-ray interactions in the atmosphere dominating the downward-going directions. Because of the high multiplicity number, these events also leave a large amount of Cherenkov photons in IceCube. This background was simulated with the CORSIKA air-shower simulation package version 6.720 [6] with the SIBYLL 2.1 [7] hadronic interaction model. Cosmic-ray interactions assuming pure proton and iron primary compositions in the energy region between 10^5 and 10^{11} GeV were simulated. EHE neutrino signal events with energies between 10^5 and 10^{11} GeV from several flux models were simulated using the JULIET package [12]. The cosmogenic neutrino induced tracks are most likely to have a near horizontal slightly downward-going geometry with falling distributions towards both vertically upward-going and downward-going directions due to the neutrino absorption in the Earth.

The simulated high energy events are divided into the shallow and deep event samples to take the difference in the optical properties of ice into account. The "depth" of the event is defined by the vertical position of the brightest photo-electron signal. The final background discrimination is performed using different sets of variables for the shallow and deep events as described in Ref. [5]. Figure 2 shows the event distributions in the planes of cos θ vs NPE for the shallow events and $\Delta\mathrm{t}_{\mathrm{LN-E}}$ vs NPE for the deep events. Here θ is the reconstructed zenith angle of the event and $\Delta\mathrm{t}_{\mathrm{LN-E}}$ is the time interval between the earliest (E) and the brightest (LN, largest NPE) photo-electron signal in the event. A clear separation between the signal and background can be observed. Reference [5] further describes the variables and compares the experimental and simulated event distributions. The straight lines and the quarter-elliptical shape show the applied NPE threshold value as a function of cos θ and $\Delta\mathrm{t}_{\mathrm{LN-E}}$, respectively. The boundaries are set such that the background expectation from cosmic-rays of an assumed pure iron primary is 0.1 events per year. For a pure proton case the background events are estimated to be at least a factor of 5 reduced from the current estimate of the background event numbers. This selection enhances the discovery potential of IceCube, which with a signal-to-background ratio of around 10 becomes quite robust against large unknown systematics uncertainties in the background estimate.

3 IceCube sensitivity beyond a PeV

The quasi-differential model-independent sensitivity of the IceCube detector at 90% CL per energy decade for neutrino fluxes above 10^{15} eV (1 PeV) is shown in Fig. 3 assuming full standard neutrino mixing. The corresponding sensitivity for a diffuse flux of cosmic neutrinos with an E^{-2} spectrum in the central 90% energy range from 300 TeV to 2 EeV is calculated to be $E^2\phi_{\nu_e+\nu_\mu+\nu_\tau} \leq 1.3\times10^{-8}\,\mathrm{GeV cm^{-2}\,sec^{-1}sr^{-1}}$ with one year of observation. The improvement of the sensitivity from the analysis of the data taken with the half completed IceCube [5] is approximately a factor of two.

Table 1 gives the event rates for several model fluxes of cosmogenic neutrinos assuming cosmic-rays to be protons only. We expect 0.8 to 1.7 cosmogenic neutrino events per year, assuming moderate to strong cosmological source evolution models, while 0.11 background events are expected in the same time period.

The corresponding neutrino effective area is shown in Fig. 4. The neutrino effective area represents the surface

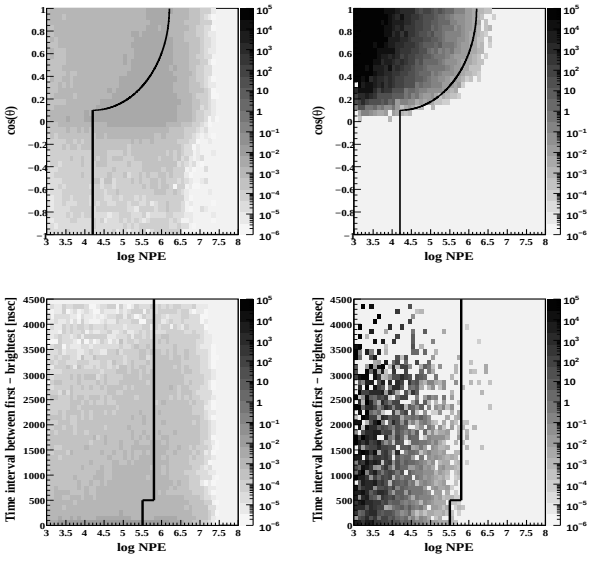

Figure 2: Event number distributions of the shallow (upper panels) and deep (lower panels) event samples in 365 days are shown for signal (left panels) and background (right panels) simulations. The signal distributions are from the cosmogenic neutrino model in Ref. [8] adding all three flavors of neutrinos. The background distributions are from CORSIKA-SIBYLL with iron primaries. The lines in each panel show the final selection criteria.

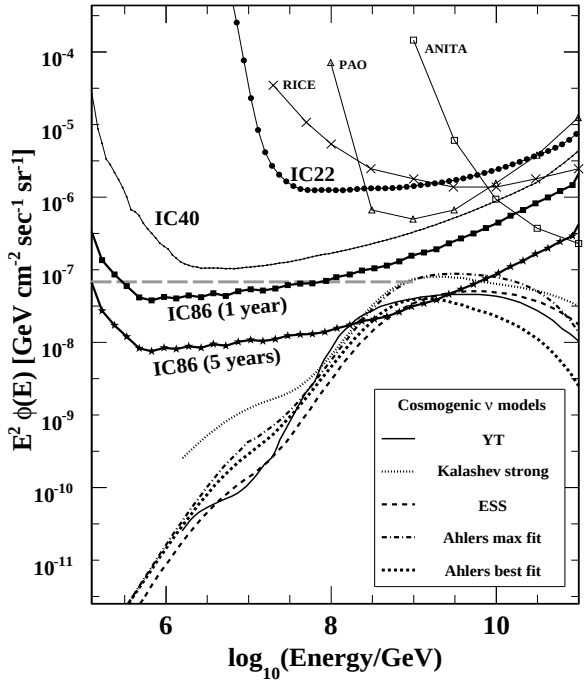

Figure 3: All flavor neutrino flux quasi-differential sensitivities of the IceCube detector after one year (filled squares) and five years (filled stars) of operations. Several model predictions (assuming primary protons) are shown for comparison: YT [8], Kalashev *et al.* (strong evolution) [9], ESS (Ω_Λ = 0.7) [10], Ahlers *et al.* (maximal), Ahlers *et al.* (the best fit, incorporating the Fermi-LAT bound) [11]. The gray dashed horizontal line indicates the Waxman-Bahcall flux bound with cosmological evolution [17]. Model fluxes are summed over all neutrino flavors, assuming standard neutrino oscillations. The model independent differential upper limits by other experiments are also shown for Auger (PAO) [13], RICE [14], ANITA [15], the previous IceCube results (2007-2008, IC22) [16], and (2008-2009, IC40) [5]. Limits from other experiments are converted to the all flavor limit assuming standard neutrino oscillation and a 90% CL per energy decade quasi-differential limit when necessary.

area of an equivalent detector if it were 100% efficient. For ν_μ and ν_τ, the areas exceed 10^3 m^2 at 10^9 GeV which is the main energy range in the IceCube cosmogenic neutrino search [5]. The present analysis is sensitive to all three neutrino flavors. Similarly the effective area near the IceCube detector can be defined as the area within which the neutrino induced muons and taus, or neutrinos are 100% detectable. They are shown in the right panel in Fig. 4. IceCube acts as a detector with effectively 50% larger volume than its actual size for neutrino-induced muons at 10^9 GeV. The effective area near the detector for the neutrinos interacting near or inside the detector (direct neutrino channel) is more than two orders of magnitude smaller than those for muons and taus. However, the direct neutrino interactions form an important contribution because the neutrino flux at IceCube depths is two orders of magnitude larger than the flux of the secondary charged leptons.

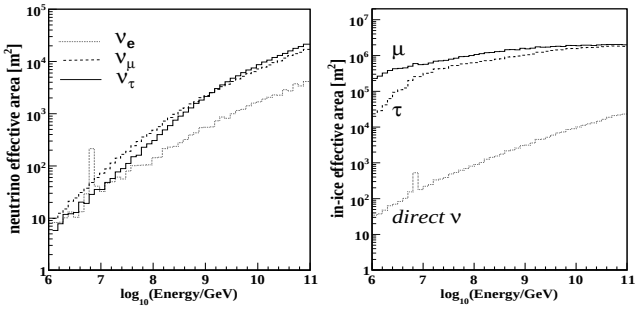

Figure 4: The left panel shows 4π solid angle averaged neutrino effective areas for each neutrino flavor. The dashed line corresponds to $\nu_e+\bar{\nu}_e$. The solid line is $\nu_\mu+\bar{\nu}_\mu$, and the dotted line is $\nu_\tau+\bar{\nu}_\tau$. All assume equal flux of neutrinos and anti-neutrinos. The right panel shows the effective detection area near the detector for secondary muons, taus and primary all flavor neutrinos.

4 Discussions

IceCube may be the first experiment to probe the cosmological evolution of the cosmic-ray sources [19].

While models of astronomical neutrinos include uncertainties in the photon field the cosmic rays interact with prior to escape from sources, CMB induced cosmogenic neutrino models are not affected by this uncertainty. Instead, these neutrino fluxes are highly dependent on the

	model parameters				Event rates
Models	m	Z_{max}	γ	E_{max}	IceCube 1 year
ESS Ω_Λ=0.7 [10]	SFR [18]	-	2.0	10^{22} eV	0.85 ± 0.01
YT [8]	4	4	2.0	10^{22} eV	1.05 ± 0.01
Kalashev *et al.* [9]	5	2	2.0	10^{22} eV	1.65 ± 0.01
Ahlers *et al.* dip transit at 10^{19} eV (best) [11]	4.6	2	2.5	10^{21} eV	0.80 ± 0.01
Ahlers *et al.* dip transit at 10^{19} eV (max.) [11]	4.4	2	2.1	10^{21} eV	1.69 ± 0.01

Table 1: Expected numbers of events by IceCube in 365 days from several cosmogenic neutrino models assuming the cosmic-ray primaries to be protons. The spectral indices γ, cutoff energies E_{max} at sources as well as cosmological evolution indices m and extensions in redshift Z_{max} for the cosmic-ray sources are also listed for reference. The corresponding expected number of background events in one year is 0.11 ± 0.01. Errors are statistical only.

cosmological distributions of the cosmic-ray sources, the cosmic-ray energy spectra in the sources, and the cosmic-ray composition. However, the cosmogenic neutrino event rates expected in IceCube are relatively stable under different assumptions on the spectra injected at the cosmic-ray sources, such as the maximum proton energy at sources and spectral indexes. Reference [9] shows that the neutrino flux significantly increases with decreasing primary spectral index from 2 to 1 only in the energy region above 10^{18} GeV. It is also shown in Ref. [10] that when the spectral index increases to 3, the neutrino spectrum is shifted to a slightly lower energy region. For both cases, only a slight increase in the event rates is expected since the target neutrino energies of IceCube are below $10^{18.5}$ eV [5]. Similarly the dependence on E_{max} is weak because it mainly affects the flux shape above 10^{18} GeV [9]. Therefore IceCube is sensitive to the redshift evolution of the co-moving density of sources, often parametrized with an exponential index m as $(1+z)^m$, to include the redshift dependence.

Studies of the baseline capability of the IceCube detector for cosmogenic neutrinos in the energy region above 1 PeV have shown that IceCube is able to detect cosmogenic neutrinos or constrain fluxes with moderate parameters, m = $3.5 \sim 4$.

In this paper we only considered the case of pure proton cosmic-ray primaries for GZK neutrino production. A detector with an order of magnitude larger fiducial volume than IceCube, such as the next generation radio Cherenkov detector arrays, ARA [20] and ARIANNA [21], is required for measurements of neutrino fluxes induced by iron-dominated cosmic-rays.

This is a performance study based on the method already realized and applied to the actual experimental data analysis [5]. New techniques are being developed for future analyses [22, 23]. For example, there is a technique to experimentally identify atmospheric muon bundle events by looking for a coincidence signature in the IceCube optical modules and the IceTop air shower surface array [22]. Differences in the energy loss profiles and waveform shapes between the atmospheric muon bundles and neutrino-induced single muon events are also being explored. These new techniques should improve sensitivities for future cosmogenic neutrino analyses with IceCube.

References

[1] K. Greisen, Phys. Rev. Lett., 1966, **16**, 748.

[2] G. T. Zatsepin and V. A. Kuzmin, Pisma Zh. Eksp. Teor. Fiz., 1966, **4**, 114 [JETP. Lett., 1966, **4**, 78].

[3] V.S. Berezinsky and G.T. Zatsepin, Phys. Lett. B, 1969, **28** 423.

[4] H. Kolanoski, IceCube summary talk, these proceedings.

[5] R. Abbasi *et al.* (IceCube Collaboration) Phys. Rev. D, 2011, **83**, 092003.

[6] D. Heck *et al.*, Report FZKA, 1998, **6019**, Forschungszentrum Karlsruhe.

[7] E. J. Ahn, R. Engel, T. K. Gaisser, P. Lipari, and T. Stanev, Phys. Rev. D, 2009, **80**, 094003.

[8] S. Yoshida and M. Teshima, Prog. Theor. Phys. 1993, **89**, 833.

[9] O. E. Kalashev, V. A. Kuzmin, D. V. Semikoz, and G. Sigl, Phys. Rev. D, 2002, **66**, 063004.

[10] R. Engel, D. Seckel, and T. Stanev, Phys. Rev. D, 2001, **64**, 093010.

[11] M. Ahlers *et al.*, Astropart. Phys. 2010, **34**, 106.

[12] S. Yoshida *et al.*, Phys. Rev. D, 2004, **69**, 103004.

[13] J. Abraham *et al.* (Pierre Auger Collaboration), Phys. Rev. D, 2009, **79**, 102001. Private communications.

[14] I. Kravchenko *et al.* (Rice Collaboration), Phys. Rev. D, 2006, **73**, 082002.

[15] P. W. Gorham *et al.* (ANITA Collaboration), Phys. Rev. D, 2010, **82**, 022004; arXiv:1011.5004 (erratum).

[16] R. Abbasi *et al.* (IceCube Collaboration), Phys. Rev. D, 2010, **82**, 072003.

[17] E. Waxman and J. Bahcall, Phys. Rev. D, 1998, **59**, 023002; S. Razzaque, P. Meszaros, and E. Waxman. Phys. Rev. D, 2003, **68**, 083001.

[18] B.J. Boyle and R.J. Terlevich, Mon. Not. R. Astron. Soc., 1998, **293**, L49-L51.

[19] S. Yoshida and A. Ishihara, paper 954, these proceedings.

[20] P. Allison *et al.*, 2011, arXiv:1105.2854

[21] L. Gerhardt *et al.*, Nucl. Instrum & Meth., 2010, **A624**, 85.

[22] J. Auffenberg, S. Cohen and K. Mase, paper 778, these proceedings.

[23] H. Wissing *et al.*, paper 949, these proceedings.

32ND INTERNATIONAL COSMIC RAY CONFERENCE, BEIJING 2011

The search for extremely high-energy neutrinos with IceCube

THE ICECUBE COLLABORATION[1]
[1]*See special section in these proceedings*

Abstract: The IceCube neutrino telescope was constructed to search for high energy neutrinos of cosmic origin. At the highest energies, neutrinos associated with the interaction of the most energetic cosmic rays with cosmic microwave background photons (GZK effect) are considered a guaranteed signal, with expected event rates of up to a few events per year in a cubic kilometer detector. Searches for GZK neutrinos have been performed using data taken with the intermediate construction stages of the now complete IceCube detector. We present the results of finished and on-going analyses, with a focus on the search using data taken between spring 2009 and spring 2010, when the IceCube detector was roughly 70% complete.

Corresponding authors: Henrike Wissing[2] *(hwissing@icecube.umd.edu)*, Aya Ishihara[3] *(aya@hepburn.s.chiba-u.ac.jp)*
[2] *University of Maryland. College Park, MD 20742, USA*
[3] *Chiba University, Chiba 263-8522, Japan*

Keywords: IceCube, GZK neutrinos, EHE neurtinos

1 Introduction

The detection of extremely-high energy (EHE) neutrinos with energies in excess of 10^7 GeV may shed light on the yet unknown origin of the highest energy cosmic rays. The direct observation of EHE charged cosmic ray particles is limited by their inevitable energy loss in the cosmic microwave background through photo-pion production, known as the Greisen-Zatsepin-Kuzmin (GZK) effect [1]. The trajectories of the charged cosmic ray particles with diminished energies will have been randomized in cosmic magnetic fields upon arrival at the Earth. Neutrinos from the decays of the secondary charged pions, $\pi^{\pm} \rightarrow \mu^{\pm}\nu_{\mu} \rightarrow e^{\pm}\nu_e\nu_{\mu}\nu_{\mu}$, will travel in straight lines and unattenuated over cosmological distances and carry information about the sources of EHE cosmic rays.

The IceCube neutrino observatory consists of a cubic kilometer sized Cherenkov detector embedded in the 2800 m thick glacial ice cap at the South Pole and an overlying square kilometer surface air-shower array. The in-ice detector consists of 5160 light sensitive digital optical modules (DOMs) deployed at depths between 1450 and 2450 m on 86 vertical cables ("strings"). Each DOM is equipped with a 25 cm photo-multiplier tube (PMT) along with two waveform digitizers and supporting data acquisition, calibration, and control hardware [2, 3]. Interactions of high energy neutrinos with the surrounding matter are detected via their Cherenkov emissions in the highly transparent Polar ice [4]. With its large detection volume, the in-ice detector is the first neutrino telescope with a realistic chance to detect the small flux of EHE neutrinos associated with the GZK effect.

During IceCube's construction phase, which started in 2005, data taken with the partially instrumented in-ice neutrino telescope have been searched for signatures of EHE neutrinos [5, 6]. The analysis of data taken during the years 2008/2009, when 40 of the 86 strings of the in-ice detector were deployed, has led to the currently most stringent limits on fluxes of EHE neutrinos with energies between 1 PeV and 10 EeV (Figure 1). In these proceedings, we report on a search for EHE neutrinos in data taken with the 59-string detector between spring 2009 and spring 2010.

2 Method

The vast majority of the events recorded by IceCube are due to down-going atmospheric muons that are created by interactions of high energy cosmic rays in the atmosphere, and which are sufficiently energetic to penetrate the ice overburden and deposit Cherenkov light in the detector. Against this background, an EHE neutrino interaction inside or in the vicinity of the detector would stand out with a much higher Cherenkov light deposition. Figure 2 shows the expected light deposition in terms of the number of recorded photo-electrons (NPE) and its correlation with the zenith angle ($\cos\Theta$) of the primary particle tracks for simulated GZK neutrino induced events and

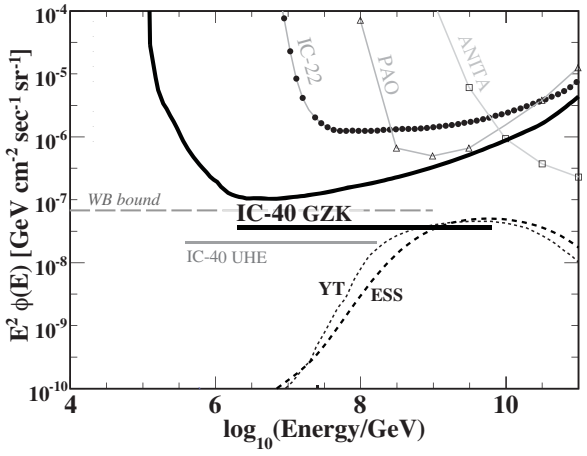

Figure 1: Present flux limits on EHE neutrinos compared to two all flavor GZK neutrino flux predictions, YT ((m, Z_{max}) = (4,4) [7] and ESS (Ω_Λ = 0.7) [8], and the Waxman-Bahcall bound [9]. Limits from IceCube 40-string GZK neutrino search (IC-40 GZK, differential limit and E^{-2} spectrum integrated limit) [6] are shown as thick black lines, the limit from an UHE neutrino search (IC-40 UHE) [10] is shown as grey horizontal line. Less stringent limits were set by Auger (PAO) [11], ANITA [12], and the IceCube 22-string detector (IC-22) [5].

simulated atmospheric background events. For both signal and background events, the light yield is strongly correlated with $\cos\Theta$. For down-going atmospheric muon events, the expected NPE rapidly decreases with increasing inclination of primary particle track, because with increasing slant depth the muons will lose more energy before reaching the detector. Below the horizon ($\cos\Theta < 0$), low energy atmospheric neutrinos arriving from the opposite hemisphere are the only expected background. The detection probability of GZK neutrinos is highest for directions close to the horizon, because of the relatively short neutrino interaction length at EHE energies.

Exploiting the correlation between the event light yield and the track direction, the data selection criteria to separate signal from background events in IceCube's EHE neutrino searches have routinely been designed as two-dimensional boundaries in the NPE-$\cos\Theta$-plane [5, 6]. Simple geometric fit methods, whose performance proved robust against systematic uncertainties in the detector response, were used to infer the track directions. In this analysis, we follow the same strategy, but we use a different fitting algorithm than previous analyses to determine the track direction.

Following a blind analysis procedure, the selection criteria are optimized on simulated signal and background events. A subset of 10% of the experimental data, evenly distributed throughout the data taking period, is used to validate the detector simulation. After the selection criteria are developed, the data selection is applied to the blinded 90% of the data, which for the 2009/2010 data-taking period roughly comprises 330 days of detector livetime. The 10% subset is discarded, in order to avoid statistical bias.

3 Monte Carlo simulations

The dominant background at the final data selection levels is high multiplicity muon bundles induced predominantly by heavy cosmic ray primaries with PeV to EeV energies. This background was simulated with the CORSIKA air-shower simulation [13] using the SIBYLL 2.1 [14] hadronic interaction model. Two primary types, proton and iron, with energies between 10^4 and 10^{11} GeV were simulated. The primaries were sampled from a power-law energy spectrum following $dN/dE \propto E^{-2}$, in oder to over-sample the high energy end of the cosmic ray spectrum, which is most important to this analysis. Proton and iron components are then re-weighted to broken power-law spectra, whose combination approximates the all particle spectrum at PeV energies and above [15].

Signal events induced by EHE neutrinos in the energy range between 10^5 and 10^{11} GeV were simulated with the JULIeT package [16]. The charged secondary particles were sampled from an energy spectrum $\propto E^{-1}$. The events can be re-weighted to various GZK neutrino flux predictions. In these proceedings, we use the predictions from references [7] and [8] (*c. f.* YT and ESS in Figure 1). The quoted event rates correspond to the sum of all three neutrino flavors, ν_e, ν_μ, and ν_τ.

4 Event selection

The first data selection for the various IceCube analyses is performed on-line at the South Pole, before data are sent to the northern hemisphere. For this analysis, the on-line filter required a minimum of 630 photo-electrons to be recorded in an event.

Following the analysis strategy that was developed for the 40-string detector [6], further data reduction is achieved by requiring at least 200 DOMs to have registered light within a time window of $[-4.4\mu s, 6.4\mu s]$ around the largest local light deposition in the detector. The latter is defined as the time at which 10% of the largest PMT pulse was captured. Further, we require the total number of photo-electrons recorded in this time window to be larger than 3200. With these requirements, the atmospheric background is reduced by two orders of magnitude, while 75% of the signal is retained (Table 1). While the previous EHE search used the *linefit* algorithm [17, 5] to reconstruct the track directions, we use a different algorithm in this analysis, the *dipolefit* [17]. The dipolefit assigns a dipole moment, $\vec{M}$, to the light pattern recorded in each event:

$$\vec{M} = \frac{1}{\frac{N_{\mathrm{DOM}}}{2}} \cdot \sum_{i=\frac{N_{\mathrm{DOM}}}{2}+1}^{N_{\mathrm{DOM}}} \frac{\vec{r}_i - \vec{r}_{i-\frac{N_{\mathrm{DOM}}}{2}}}{|\vec{r}_i - \vec{r}_{i-\frac{N_{\mathrm{DOM}}}{2}}|}, \qquad (1)$$

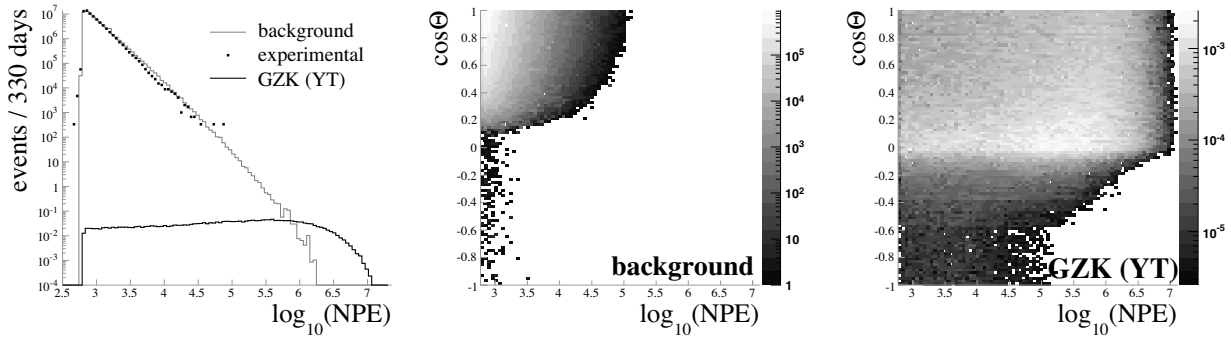

Figure 2: Expected light yield (logarithm of the number of detected photoelectrons, $\log_{10}(NPE)$), for simulated signal and background events and a subset of the experimental data set (left) and the correlation with the cosine of the zenith angle of the primary particle tracks for simulated atmospheric background events (middle) and GZK neutrinos (right). The background prediction includes cosmic ray induced muons, assuming a cosmic ray spectrum according to [15], and atmospheric neutrinos according to [18] with a contribution from prompt neutrinos according to [19]. The GZK neutrino spectrum is simulated according to [7] (*c. f.* YT in Figure 1).

cut	Experimental	Background	GZK YT [7]	GZK ESS [8]
$NPE > 630$	6.20×10^7	$(6.86 \pm 0.18) \times 10^7$	2.35 ± 0.01	1.81 ± 0.01
$NPE > 3200$ and $N_{\mathrm{DOM}} > 200$	6.65×10^5	$(7.68 \pm 0.12) \times 10^5$	1.80 ± 0.01	1.38 ± 0.01
$\log_{10}(NPE) - 0.5 \cdot \mathcal{D} > 4$	336	365 ± 6	1.39 ± 0.01	1.07 ± 0.01

Table 1: Expected event rates at various selection levels for 330 days of detector livetime. The signal rates correspond to the GZK neutrino models according to [7] (YT) and [8] (ESS). Errors are statistical only.

where $\vec{r}_i$ is the vector of spatial coordinates of the DOM that recorded the ith light signal in time, and N_{DOM} is the total number of DOMs fired in the event. The magnitude of the dipole moment $|\vec{M}|$ takes values between 0 and 1, and provides a measure for the directionality of the light flow in the event: large values of $|\vec{M}|$ indicate a track-like signal, while small values indicate a rather spherical light pattern. EHE neutrino interactions typically yield small dipole moments. Cascades induced by ν_e and ν_τ interactions naturally generate spherical light patterns, and the light pattern from ν_μ induced EHE muons has a broad radial distribution. Low energy atmospheric muon events on the other hand, typically have dipole moments close to 1.

Figure 3 shows the correlation between the magnitude and the direction ($\cos\Theta_{\mathrm{M}}$) of the dipole moment for atmospheric background events and GZK neutrino signal. Background events cluster in the region with large dipole moments and down-going directions. A combination of both magnitude and direction of the dipole moment, $\mathcal{D} = \cos\Theta_{\mathrm{M}} + 2 \cdot |\vec{M}|$, is used as a measure of the similarity of an event to a down-going track. Compared to a cut on the reconstructed direction only, a larger fraction of the extremely bright EHE neutrino signal events is preserved.

Background events with low values of $\mathcal{D}$ are predominantly induced by low energy neutrinos and atmospheric muons that pass outside the instrumented volume and deposit only very little Cherenkov light. Figure 4 shows the correlation of $\mathcal{D}$ with the light yield NPE. Signal and background events are well separated in the $\mathcal{D}$-NPE-plane. A two-dimensional cut in this plane defined by $(\log_{10}(NPE) - 0.5 \cdot \mathcal{D}) > 4$ reduces the atmospheric background by two more orders of magnitude, while the expected GZK neutrino signal still exceeds one event in 330 days (Table 1).

Additional selection criteria to separate the GZK signal events from the remaining background are being investigated. A realistic chance to detect a GZK neutrino signal requires the further selection criteria to keep the signal expectation above 1 event, while suppressing the background to a level of $\mathcal{O}(0.1)$ expected events per year. The GZK neutrino search with the 40-string detector [6] achieved a signal expectation of 0.5 events for GZK models presented here, above an expected background of roughly 0.1 events at the final selection level. With the larger 59-string detector, improved event selection criteria, and better understanding of the detector response, the required signal to background ratio to either detect GZK neutrinos or to constrain the here considered flux predictions seems within reach.

5 Conclusions

The detection of GZK neutrinos with IceCube seems tantalizingly close. The analysis of data taken with an intermediate construction stage of the detector, in which half the in-ice detector was deployed, allowed to place the most stringent limits on EHE neutrinos to-date. Data taken with later construction stages are presently being analyzed. Al-

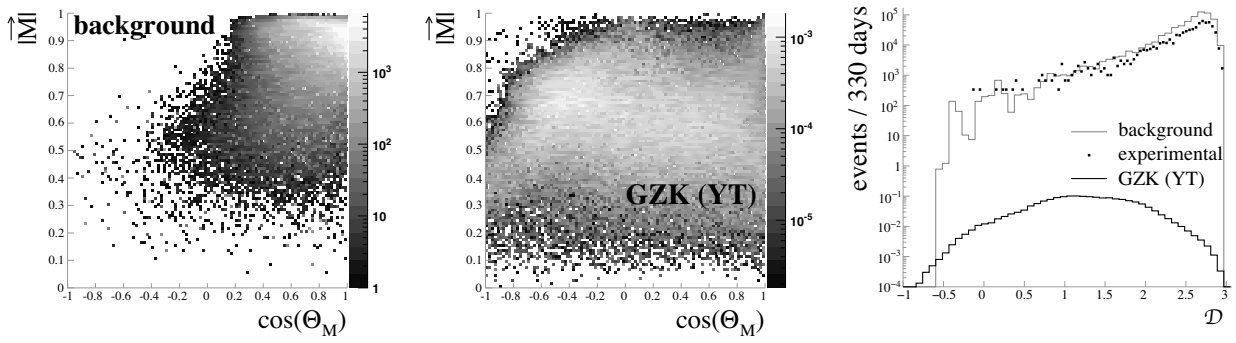

Figure 3: Observables of the *dipolefit*. The magnitude of the dipole moment $|\vec{M}|$ versus the reconstructed zenith angle ($\cos\Theta_{\rm M}$) for simulated background events (left) and simulated signal events (middle). The linear combination $\mathcal{D} = \cos\Theta_{\rm M} + 2 \cdot |\vec{M}|$ (right), is a measure the similarity of the event to a down-going track.

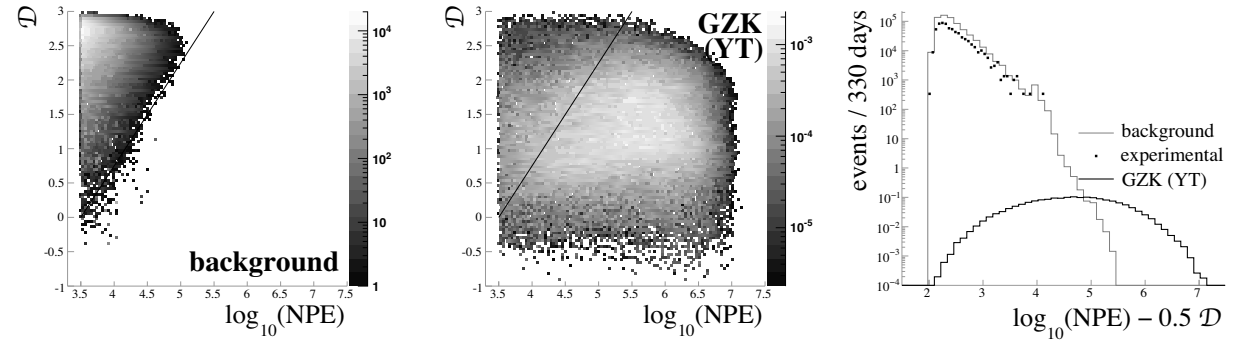

Figure 4: Correlation of the combined dipole observable $\mathcal{D} = \cos\Theta_{\rm M} + 2 \cdot |\vec{M}|$ with NPE for simulated background events (left) and simulated signal events (middle). The linear combination of $\mathcal{D}$ and NPE that is used as a cut parameter is shown in the right panel. The separating boundary defined by $\log_{10}(NPE) - 0.5 \cdot \mathcal{D} > 4$ is shown as black lines in the two dimensional plots.

ready the next construction stage, which roughly 70% of the detector components deployed, may reach the sensitivity to probe current models of GZK neutrino fluxes.

References

[1] K. Greisen, Phys. Rev. Lett. **16**, 748 (1966). G. T. Zatsepin and V. A. Kuzmin, Pisma Zh. Eksp. Teor. Fiz. **4**, 114 (1966) [JETP. Lett. **4**, 78 (1966)].

[2] R. Abbasi *et al.* (IceCube Collaboration), Nucl. Instrum. Meth. **A618**, 139 (2010).

[3] R. Abbasi *et al.* (IceCube Collaboration), Nucl. Instrum. Meth. **A601**, 294 (2009).

[4] M. Ackermann *et al.* (IceCube Collaboration), J. Geophys. Res. **111**, D13203 (2006).

[5] R. Abbasi *et al.* (IceCube Collaboration), Phys. Rev. **D82**, 072003 (2010).

[6] R. Abbasi *et al* (IceCube Collaboration), Phys. Rev. **D83**, 092003 (2011).

[7] S. Yoshida and M. Teshima, Prog. Theor. Phys. **89**, 833 (1993).

[8] R. Engel, D. Seckel, and T. Stanev, Phys. Rev. **D64**, 093010 (2001).

[9] E. Waxman and J. Bahcall, Phys. Rev. **D59**, 023002 (1999). S. Razzaque, P. Meszaros, and E. Waxman, Phys. Rev. **D68**, 083001 (2003).

[10] H. Johansson, PhD Thesis, Stockholm University, Sweden (2011).

[11] J. Abraham *et al.* (Pierre Auger Collaboration), Phys. Rev. **D79**, 102001 (2009).

[12] P. W. Gorham *et al.* (ANITA Collaboration), Phys. Rev. **D82**, 022004 (2010); arXiv:1011.5004 (erratum).

[13] D. Heck *et al.*, Report FZKA **6019** (Forschungszentrum Karlsruhe 1998).

[14] E. J. Ahn, R. Engel, T. K. Gaisser, P. Lipari, and T. Stanev, Phys. Rev. **D80**, 094003 (2009).

[15] R. Glasstetter *et al.*, Proc. 26th ICRC, Salt Lake City, USA (1999).

[16] S. Yoshida *et al.*, Phys. Rev. **D69**, 103004 (2004).

[17] J. Ahrens *et al.* (IceCube Collaboration), Nucl. Instrum. Meth. **A524**, 169 (2004).

[18] M. Honda *et al.*, Phys. Rev. **D75**, 043006 (2007).

[19] E. Bugaev *et al.*, Phys. Rev. **D58**, 054001 (1998).

32ND INTERNATIONAL COSMIC RAY CONFERENCE, BEIJING 2011

New Background Rejection Methods for the GZK Neutrino Search with IceCube

THE ICECUBE COLLABORATION[1]
[1] *see special section in these proceedings*

Abstract: The detection of cosmogenic (GZK) neutrinos with IceCube requires the ability to discriminate very rare and energetic signal events from an abundant background of cosmic ray induced muons. High energy cosmic ray air showers produce high numbers of muons densely packed around the shower core trajectory. These bundles of muons emit large amounts of Cherenkov light in the ice that constitutes the detection volume. We present several techniques to improve background rejection while keeping a large fraction of the GZK neutrino signal. The differences in the light distributions around a neutrino-induced muon track and a muon bundle are exploited. The photon hit-time pattern in the detector differs slightly for the two event types and is used for identification of muon bundles. The surface array, IceTop, is used to tag the background with high efficiency but limited zenith range. The efficiency of this method was studied using data from the partially completed detector.

Corresponding authors: Jan Auffenberg[2] (*jan.auffenberg@icecube.wisc.edu*),
Shirit Cohen[3] (*shirit.cohen@icecube.wisc.edu*), Keiichi Mase[4] (*mase@hepburn.s.chiba-u.ac.jp*)
[2]*University of Madison Wisconsin, 222 W. Washington, Madison, USA*
[3]*Laboratory for High Energy Physics, École Polytechnique Fédéral, CH-1015 Lausanne, Switzerland*
[4]*Chiba University, Yayoi-cho 1-33, Inage-ku, Chiba-shi, Chiba, Japan*

Keywords: UHECR; GZK neutrinos; IceCube

1 Introduction

Ultra High Energy Cosmic Rays (UHECRs) with energies above 10^{11} GeV have been observed by several experiments[1, 2]. The origin of UHECRs remains unknown, though there may be indications of a correlation of incoming directions with the close-by extra-galactic source distribution [3]. The elucidation of the origin has been longed for from the first detection. UHECRs interact with cosmic microwave background photons and necessarily generate neutrinos with energies in excess of 10^7 GeV through secondary pion decays (GZK effect). Therefore, the detection of such Extremely High Energy (EHE) neutrinos can shed light on the UHECR origin.

The IceCube detector [4], completed in Dec. 2010, instruments a huge volume of 1 km^3 ultra transparent glacial ice and is suitable to search for rare EHE neutrino events.

The GZK neutrino flux prediction depends on the cosmological source evolution, the source injection spectra and the cosmic ray composition [5]. The expected GZK neutrino event rate in IceCube is about one event per year [5, 6].

The main background for EHE neutrino search comes from muon bundles induced by cosmic ray interactions in the atmosphere. While bundles are much more abundant compared to the expected neutrino signal, their flux decreases steeply with increasing energy. Therefore signal, expected to have a harder energy spectrum, may emerge from the background above a certain critical energy. In addition, muon multiplicity in bundles increases with the primary cosmic ray energy, which leads to more pronounced background-event signatures and to increasing rejection efficiency. Another difference between neutrinos and muon bundles is their arrival direction. While the muon bundle rate decreases with increasing zenith angle, near horizontal directions are favored for GZK events because of the increase of the neutrino cross section at high energies.

The energy and arrival direction information has been used in several EHE neutrino searches [7, 8] producing the best upper limit for EHE neutrinos in the relevant energy range around 10^9 GeV.

In this paper we present methods which are being developed to achieve higher signal efficiency and high-multiplicity muon bundle background rejection using the characteristic differences between the two.

2 Muon Bundle Rejection Techniques

In Extensive Air Showers (EAS), more than thousands of muons can be generated and reach the IceCube detector

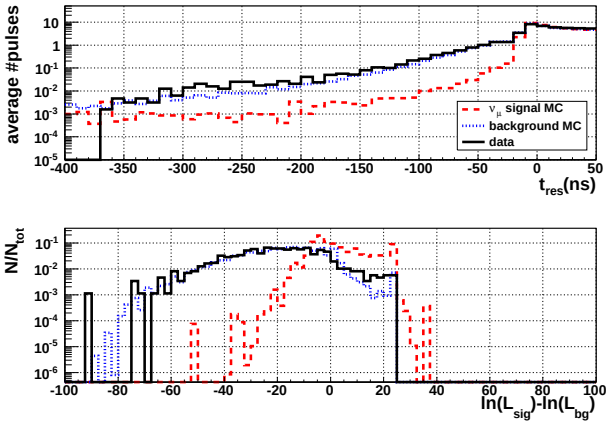

Figure 1: Top: Average number of recorded pulses as a function of the time residual for events with 10,000 <NPE< 30,000. Bottom: negative time residual likelihood ratio distribution for the same events. Dashed red: ν_μ signal simulation, dotted blue: background simulation, black: experimental data.

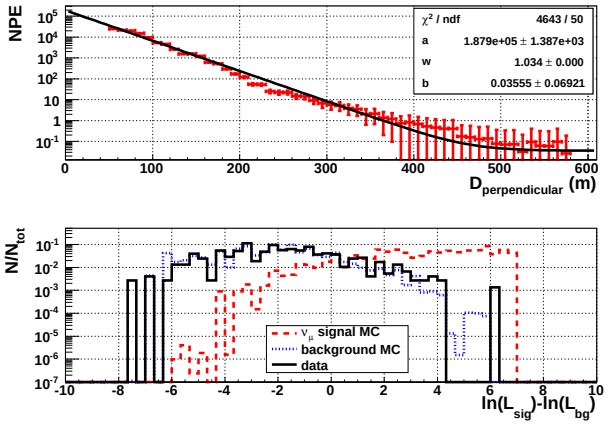

Figure 2: Top: Distribution of detected light perpendicular to a simulated neutrino-induced single muon track (red markers) and the fitted μ function (black) for an event with 100,000 NPE. Bottom: light distribution likelihood parameter ratio distribution for events with 10,000 < NPE < 30,000.

depth, under an ice overburden of about 1500 m. Most of these muons are concentrated in a dense core, but some may have relatively high transverse momenta p_t and are therefore separated from the core of the bundle at the depth of IceCube by a distance $\propto p_t/E_\mu$. Multiple scattering and deflection due to the Earth's magnetic field can increase the separation for near-horizontal events [9]. Observing the separation of single muons within the bundle core is not possible in IceCube as the photon scattering length in ice is too short and the detector's string spacing is too large for this purpose. However, differences in the light distribution around the bundle core compared to that around a single muon can be used to distinguish the two event classes.

2.1 Early Photon Hit Times

The application of a single muon hypothesis track reconstruction [10] to a muon bundle event gives the location and direction of the bundle axis. For each detected Digital Optical Module (DOM) pulse and a given reconstructed track we define the time residual $t_{\rm res}$ as the difference between the measured pulse time and the expected arrival time of an unscattered Cherenkov photon from the single track hypothesis. In the muon bundle case, the light generated by outlying muons may result in pulses with negative $t_{\rm res}$ values, indicating photon arrival times inconsistent with the single track hypothesis. We exploit the density of negative $t_{\rm res}$ pulse distribution by means of a likelihood analysis where signal and muon bundle background hypotheses are compared. The distribution of number of pulses with negative $t_{\rm res}$ values for simulated signal and background, compared to experimental data events for the IceCube 40 string configuration is shown in Fig. 1 (top). The observable NPE refers to the total Number of Photo-Electrons collected in an event by the IceCube DOMs. The resulting likelihood parameter distributions are shown in Fig. 1 (bottom).

2.2 Perpendicular Light Distribution

The amount of detected light at perpendicular distances from a single muon track is a function of the muon energy, ice properties and the detector noise level due to DOM electronics. Its parameterization is described in [11] and is given by

$$\mu(d,\theta,E) = a(\theta,E)\,\omega^{-d/d_0} + b_{\rm noise} \qquad (1)$$

with d: DOM-track distance, θ: string axis-track opening angle, E: energy of the track and $d_0 = 1$ m. Parameter a (in units of NPE) represents the light normalization and is dependent on energy of the track in IceCube, the dimensionless parameter ω describes the shape of the falling light curve and $b_{\rm noise}$ (in units of NPE) gives the expected noise level of the DOMs. Parameters a and ω are both dependent on ice properties which vary with depth [12]. However, it is difficult to resolve the dependency as for each event light is emitted and detected at different ice depths and the dependency is averaged in the fitted parameter values.

Examples for the detected light distribution around a single muon neutrino event and the fitted $\mu(d,\theta,E)$ function are given in Fig. 2 (top). The radial spread of the muons inside the bundle can be up to ~ 50 m, so the perpendicular light distribution at small distances is flatter around a bundle compared to a single muon track. The amount of detected light at larger distances is higher for a single muon track compared to a bundle. This could be because muons in the bundle range out and do not reach the clearest ice at the bottom of the detector and because of large stochastic energy losses in the single muon case. These differences appear mostly in the value of the fitted ω parameter. For

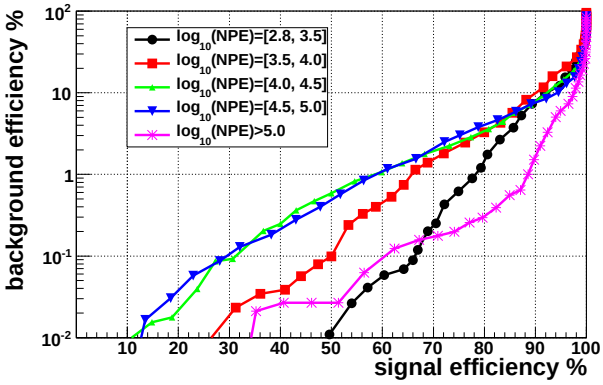

Figure 3: Combined $\Delta \ln(L)$ cut signal efficiency vs. background efficiency. For a signal cut efficiency of 90% the background rejection efficiency ranges from 90%-98% for neutrino energies of $10^{6.5} - 10^{11}$ GeV. The curves refer to samples of events with increasing amount of light detected with the IceCube 40 string detector.

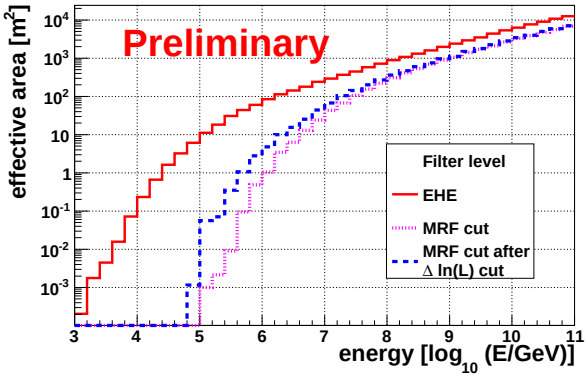

Figure 4: ν_μ effective areas for a simple analysis using a combined $\Delta \ln(L)$ cut on MC simulation of IceCube 40 string configuration. Full red: IceCube EHE events filter level, dotted purple: MRF cut calculated on filter level event sample, dashed blue: MRF cut calculated after applying a combined $\Delta \ln(L)$ cut.

signal and background events in a GZK neutrino search the obtained 2-dimensional distributions of fitted ω versus a values occupy different areas of the phase space. A likelihood parameter comparing signal and muon bundle background hypotheses is constructed and its distributions for the IceCube 40 string configuration simulated and experimental data events are shown in Fig. 2 (bottom).

2.3 Results

The bundle rejection observables described in sections 2.1 and 2.2 were combined in a single likelihood parameter. Background vs signal efficiency is shown in Fig. 3 as a function of a cut on the combined likelihood ratio $\Delta \ln(L)$ defined as $\ln(L_{\rm sig}) - \ln(L_{\rm bg})$. In order to assess the strength of the combined $\Delta \ln(L)$ observable, a cut was set at a fixed $\Delta \ln(L)$ value which gives signal passing rates of $88\% - 97\%$ depending on NPE range. A signal selection NPE threshold was then calculated using the MRF technique [14] on simulated and experimental data that passed both the EHE event filter (NPE > 630) and the combined $\Delta \ln(L)$ cut. The resulting effective areas are shown in Fig. 4.

3 IceTop Veto on Cosmic Ray Showers

An EAS event in the IceCube detector may be preceded by hits recorded in the surface detector IceTop. Therefore another promising technique to discriminate muon bundles from EHE neutrinos is to use IceTop to veto muon bundles. IceTop uses the same DOMs as IceCube to detect the electromagnetic and muonic part of EAS. For the IceTop veto the electromagnetic part plays only a minor role. Inclined EAS are mostly tagged by detection of high p_t muons far away from the shower core.

An efficient IceTop veto against high energy EAS will improve the signal efficiency in a GZK neutrino search. The three main parameters determining the EAS veto efficiency are:

Primary Energy and Composition: The higher the primary energy of the EAS, the higher the probability to see a signal in IceTop, as the number of secondary particles and the lateral extension increases. A higher veto probability for heavier primary particles is expected due to more secondaries.

Distance to IceTop: The shorter the distance of the shower core from IceTop, the higher the probability to detect the event by IceTop. The distance of the shower core can be up to several km, depending on the geometrical hit position in IceCube. This parameter is closely related to the inclination.

Inclination: With increasing inclination the air shower propagates through more atmosphere where the electromagnetic shower component gets attenuated more than the hadronic component. Thus for near-horizontal showers we expect IceTop to detect mainly muons.

Single tank hits in IceTop are used to establish the IceTop veto [13]. These IceTop hits have to be within the time window of several μs of a high energy event that triggered IceCube. In order to find hits in coincidence with the air shower front, we reconstruct the shower front in time and space. Here the center of gravity of the IceCube event and the direction from the track reconstruction are used. A planar shower front is a good approximation to find coincident hits and can be corrected by a parameterization of the shower front curvature. Fig. 5 shows the principal idea of the IceTop veto.

The distribution in Fig. 5 is used to fix the size of the veto time window to 400 ns covering the coincidence peak. For comparison, we take a background time window of the

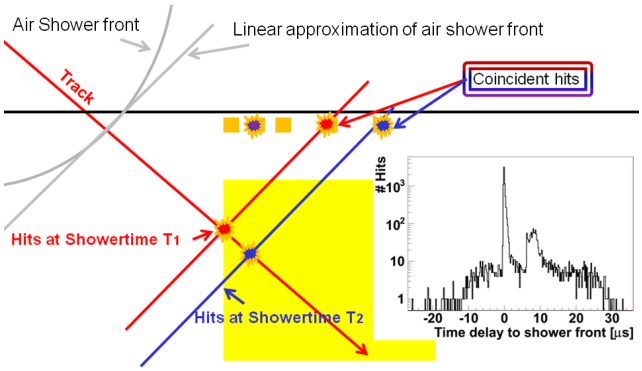

Figure 5: Sketch illustrating the veto principle. The right plot shows the IceTop hit distribution over time relative to the shower front. The sharp peak at $T = 0$ in the plot is caused mainly by coincident IceTop hits. The second peak after the shower front has passed is caused by after-pulses of the photomultipliers.

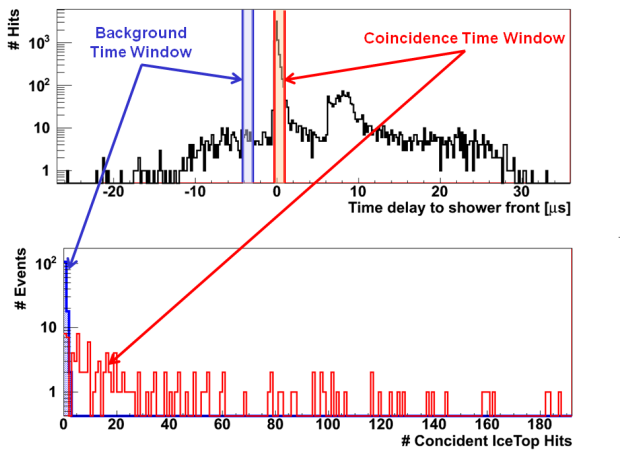

Figure 6: Top: Illustration of the chosen coincidence time windows for events with NPE $>$ 30,000. The background time window contains hits due to background from uncorrelated cosmic ray showers. Bottom: The number of events in the background time window falls steeply as a function of IceTop hits. The distribution for events in the coincidence window is significantly flatter, indicating a preliminary veto efficiency higher than 85% for NPE $>$ 30,000.

same length before the shower front reaches IceCube so that only hits from uncorrelated cosmic ray showers are included. The upper plot of Fig. 6 shows the time window selection strategy. The lower plot shows the number of events as a function of hits for both the random and real coincidence time windows. The ratio of the number of events in the real coincidence time window over the number of events in the random coincidence time window for a given number of hits gives the probability of the event to have correlated hits. Due to the low statistics of the available test data (10% of IceCube data taken in 2010 with 79 string configuration), no detailed systematic analysis of the veto efficiency is possible yet. The random coincident background is following Poisson statistics and is independent of the coincident hits. We assume that our data contains exclusively cosmic ray induced events and neglect all other background contributions. Estimates of the veto efficiency have to take into account the full dependences on energy, inclination, and distance to IceTop. All events with an NPE value exceeding 10^5 in the IceCube 2010 test data fulfill the 99.99% coincidence probability (5 hits in the coincidence time window). We conclude that the high veto efficiency at very high energies makes the IceTop veto a powerful instrument for GZK and diffuse neutrino searches.

4 Possible Future Improvements

Other variables are under investigation with the aim of further improving the sensitivity to EHE neutrinos. The longitudinal distribution of the amount of detected photons has been found to differ between a single muon derived from a neutrino and muon bundles [15]. The observed distribution along muon bundles is rather smooth while the one around single muons fluctuates much more and exhibits DOMs that detect very low PE values, which do not exist in the bundle case. It is important to separate EHE neutrinos passing far away from the detector center from the abundant lower energy muon bundles passing well within the fiducial detector volume since both of them yield similar NPE. Time-over-threshold of the recorded charge for each DOM was found to be a good proxy for the distance of light source from the DOM. This information will be used in a future EHE neutrino search as well as utilizing the IceTop veto power.

References

[1] R. Abbasi et al., Astropart. Phys., 2009, **32**: 53-60.
[2] J. Abraham et al., Phys. Lett. B, 2010, **685**: 239-246.
[3] P. Abreu et al., Astropart. Phys., 2010, **34**: 314-326.
[4] H. Kolanoski, IceCube summary talk, these proceedings.
[5] IceCube Collaboration, paper 0773, these proceedings.
[6] IceCube Collaboration, paper 0949, these proceedings.
[7] R. Abbasi et al., Phys. Rev. D, 2010, **82**: 072003.
[8] R. Abbasi et al., Phys. Rev. D, 2011, **83**: 092003.
[9] L. Gerhardt et al., Proceedings of the 31st ICRC, Lodz, Poland, July 2009. arXiv:0909.0055v.1.
[10] J. Ahrens et al., Nucl. Inst. Meth., 2004 **A524**: 169-194.
[11] M. Ribordy, Nucl. Inst. Meth., 2007, **A574**: 137-143.
[12] M. Ackermann et al., J. Geophys. Res., 2006, **111**: D13203.
[13] R. Abbasi et al., Nucl. Inst. Meth. A, 2009, **601**: 294-316.
[14] G. Hill et al., Astropart. Phys., 2003, **19**: 393-402.
[15] IceCube Collaboration, paper 0085, these proceedings.